Electronic Supplementary Information

Reversible Disassembly of Metallasupramolecular Structures Mediated by a Metastable-State Photoacid

Suzanne M. Jansze, Giacomo Cecot, and Kay Severin

Institut des Sciences et Ingénierie Chimiques, Ecole Polytechnique Fédérale de Lausanne (EPFL), 1015 Lausanne, Switzerland

Table of Contents

1. General

All chemicals were obtained from commercial sources (see below) and used without further purification unless stated otherwise. Solvents were dried using a solvent purification system from Innovative Technologies, Inc.. Reactions were carried out under an atmosphere of dry N_2 using standard Schlenk techniques. The Pd^{II} complex [(dppp)Pd(OTf)$_2$],[S1]and the metallasupramolecular structures **5**,[S2] **7**,[S3] **8**,[S3] **9**,[S4] and **10**[S5] were prepared accoring to literature procedures.

Commercial sources: 2,2'-Dipyridyl – TCI; 2,4,6-Tri(4-pyridyl)-1,3,5-triazine – ABCR; Iron(II) tetrafluoroborate hexahydrate – Sigma Aldrich; Pyridine – Sigma Aldrich; Sodium Tetrakis(4-fluorophenyl)borate Hydrate – TCI; Tetrakis(acetonitrile)-palladium(II) tetrafluoroborate – ABCR; Zinc tetrafluoroborate hydrate – ABCR

NMR spectra were obtained on a Bruker DRX (^{1}H: 400 MHz, ^{13}C: 100 MHz) equipped with a BBO 5 mm probe, a Bruker Avance III spectrometer (^{1}H: 600 MHz) equipped with a 5 mm CPTCIz cryo-probe and a Bruker Avance III spectrometer (^{1}H: 400 MHz) equipped with a 5 mm BBFO-Plus probe.

The chemical shifts are reported in parts per million δ (ppm) referenced to the residual solvent signal, unless stated otherwise. All spectra were recorded at 298 K, unless stated otherwise. The analysis of NMR spectra was performed with MestreNova and for the DOSY analysis the Baysian DOSY transform from MestreNova was used.

Routine ESI-MS data were acquired on a Q-TOF Ultima mass spectrometer (Waters) operated in the positive ionization mode and fitted with a standard Z-spray ion source equipped with the Lock-Spray interface. Data were processed using the MassLynx 4.1 software.

High resolution mass spectra were acquired for pure, pre-synthesized samples of all cages. The analytes were diluted in acetonitrile to a final concentration of ~10-20 μM. High resolution mass spectrometry experiments were carried out using a hybrid ion trap-Orbitrap Fourier transform mass spectrometer, Orbitrap Elite (Thermo Scientific) equipped with a TriVersa Nanomate (Advion) nano-electrospray ionization source. Mass spectra were acquired with a minimum resolution setting of 120,000 at 400 m/z. To reduce the degree of analyte gas phase reactions leading to side products unrelated to solution phase, the transfer capillary temperature was lowered to 50 °C. Experimental parameters were controlled via standard and advanced data acquisition software. Post-acquisition analysis was performed using vendor software, Xcalibur (Thermo Scientific), and ChemCalc (http://www.chemcalc.org/) web tool.[S6]

2. Experimental set-up for the photoswitching experiments

The photoswitching experiments were performed with the use of a Topled (MDE Display + Electronics GmbH) SET5050-5M-RGB wrapped around a glass container (see image below). To activate the photoacid, the samples were placed in the container and irradiated with violet light (425 nm) for 20 minutes at r.t., unless stated otherwise. The samples are then left at r.t. in the dark for the indicated time.

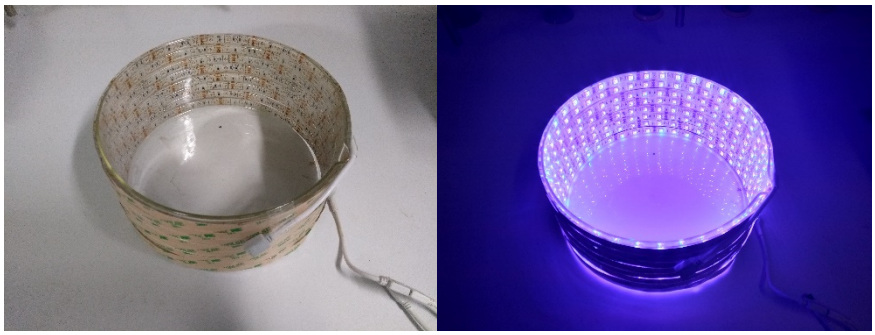

Figure S1. Experimental set-up for the activation of the photoacid. On the photo on the left side, the LEDs are turned off, and on the photo on the right side, they are turned on with the same violet light that was used for these experiments.

The CD_3CN/D_2O (8:2) solvent mixture was suited to solubilize the photoacid and a range of metallasupramolecular structures. All samples were prepared using 2 mg of photoacid (5 µmol in 0.5 mL, 1 mM). The amount of the metallasupramolecular assembly was adjusted to the amount of the photoacid. We used 4 equivalents of photoacid per functional group that can be protonated (so in most cases, per pyridine group). For example: the octahedral cage **5** has 12 ligands, with 2 pyridine groups per ligand, so (2x12=) 24 times 4, comes to 96 equivalents of photoacid with respect to the amount of **5**. The samples were prepared and handled in the dark unless stated otherwise.

3. Synthetic procedures and characterization

3.1. Model complexes (1–4)

General procedure for the synthesis of model complexes (**1**–**4**).

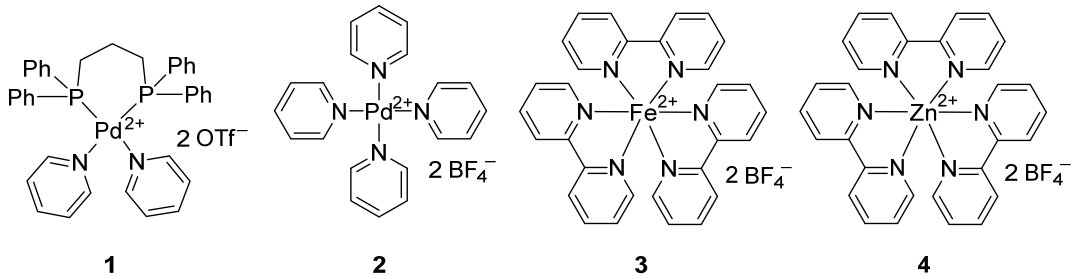

1 **2** **3** **4**

Figure S2. Chemical structures of model complexes **1**–**4**.

For the amounts and metal (complex) source used, see the table below.

Pyridine (5 mg, 0.06 mmol) (for **1** and **2**) or 2,2'-bipyridine (30 mg, 0.19 mmol) (for **3** and **4**) was combined with the corresponding metal (complex) in degassed acetonitrile (5 mL). The mixture was stirred at r.t. for 18 h, after which diethyl ether (10 mL) was added to precipitate the complex. The solid was collected by centrifugation and washed with diethyl ether (10 mL) to obtain the complexes **1**–**4**.

Model complexes

Model complex #	Metal complex	Equivalents of ligand to metal	mg	Yield
1	$(dppp)Pd(OTf)_2$	2	15.3	18.2 mg, 60%
2	$Pd(CH_3CN)_4(BF_4)_2$	4	7.0	8.3 mg, 88%
3	$Fe(BF_4)_2 \cdot 6H_2O$	3	14.7	42.2 mg, 93%
4	$Zn(BF_4)_2 \cdot 6H_2O$	3	20.0	34.4 mg, 91%

Table S1. Amounts used, and yield for the synthesis of model complexes **1**–**4**.

Characterization of model complexes **1**–**4**.

1: ^{1}H NMR (400 MHz, $CD_3CN:D_2O$ 4:1) δ = 8.42 (d, J=5.3, 4H), 7.69 – 7.07 (m, 26H), 2.92 (broad s, 2H), 2.16 (tr, J=18, 4H). ^{13}C NMR (151 MHz, $CD_3CN:D_2O$ 4:1) δ 150.62, 140.23, 133.83, 133.77, 133.63, 130.53, 130.45, 127.17, 122.42, 22.29, 18.45.^{31}P NMR (162 MHz, $CD_3CN:D_2O$ 4:1) δ 8.2. HRMS (ESI): *m/z* calculated for $C_{37}H_{36}N_2P_2Pd$ $[M\text{-}2OTf]^{2+}$ 338.0689, found 338.0696

2: ^{1}H NMR (600 MHz, $CD_3CN:D_2O$ 4:1) δ = 8.80 (d, J=5.1, 8H), 7.95 (t, J=9.0, 4H), 7.51 (d, J=6.6, 8H). ^{13}C NMR (151 MHz, $CD_3CN:D_2O$ 4:1) δ = 152.00, 142.07, 128.39. HRMS (ESI): *m/z* calculated for $C_{20}H_{20}N_4Pd$ $[M\text{-}2BF_4]^{2+}$ 211.0356, found 211.0360.

3: ^{1}H NMR (600 MHz, $CD_3CN:D_2O$ 4:1) δ = 8.52 (d, J=6.0, 6H), 8.07 (t, J=6.0, 6H), 7.36 (m, 12H). ^{13}C NMR (151 MHz, $CD_3CN:D_2O$ 4:1) δ 160.04, 154.97, 139.67, 128.34, 124.86. HRMS (ESI): *m/z* calculated for $C_{30}H_{24}N_6Fe$ $[M\text{-}2BF_4]^{2+}$ 262.0700, found 262.0700.

4: ^{1}H NMR at 275K (400 MHz, $CD_3CN:D_2O$ 4:1, 275 K) δ = 8.51 (d, J=8.1, 6H), 8.21 (t, J=7.8, 6H), 7.90 (d, J=2.4, 6H), 7.53 (t, J=8.1, 6H). ^{13}C NMR (151 MHz, $CD_3CN:D_2O$ 4:1) δ = 150.10, 148.97, 142.80, 128.39, 124.24. HRMS (ESI): *m/z* calculated for $C_{30}H_{24}N_6Zn$ $[M\text{-}2BF_4]^{2+}$ 266.0671, found 266.0674.

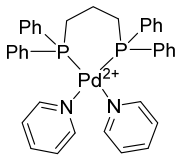

1

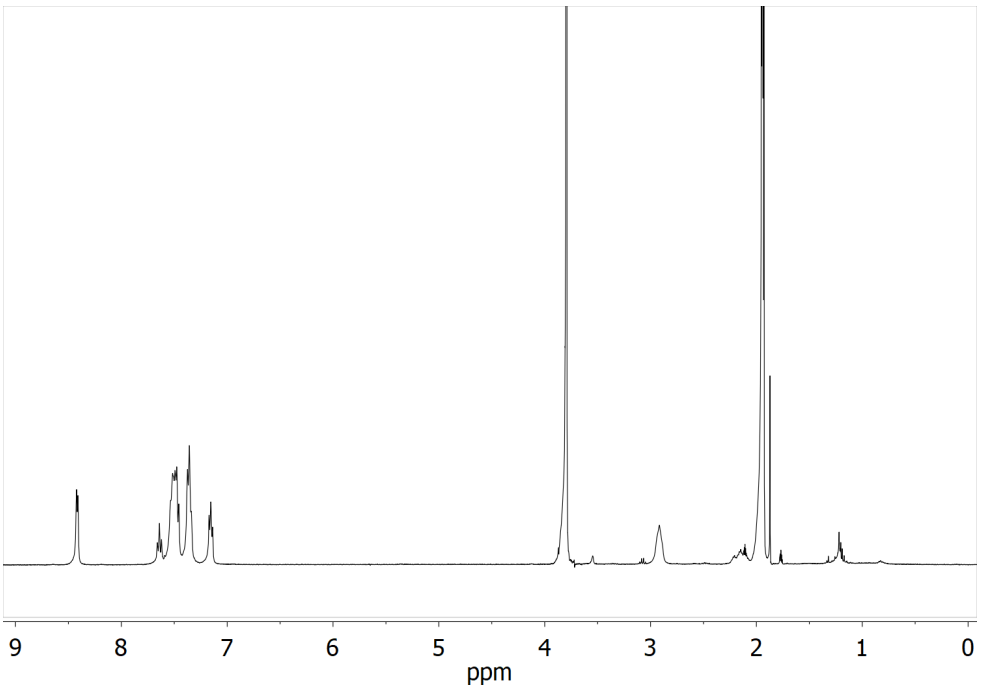

Figure S3. ^{1}H NMR spectrum of complex **1** in an 80/20 mixture of CD_3CN and D_2O.

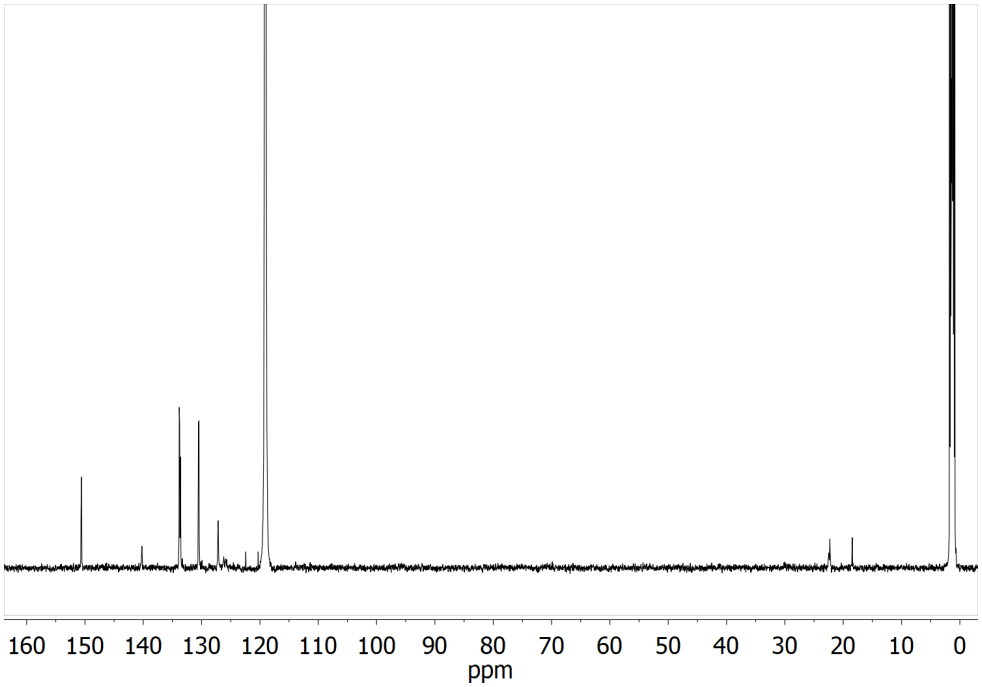

Figure S4. ^{13}C NMR spectrum of complex **1** in an 80/20 mixture of CD_3CN and D_2O.

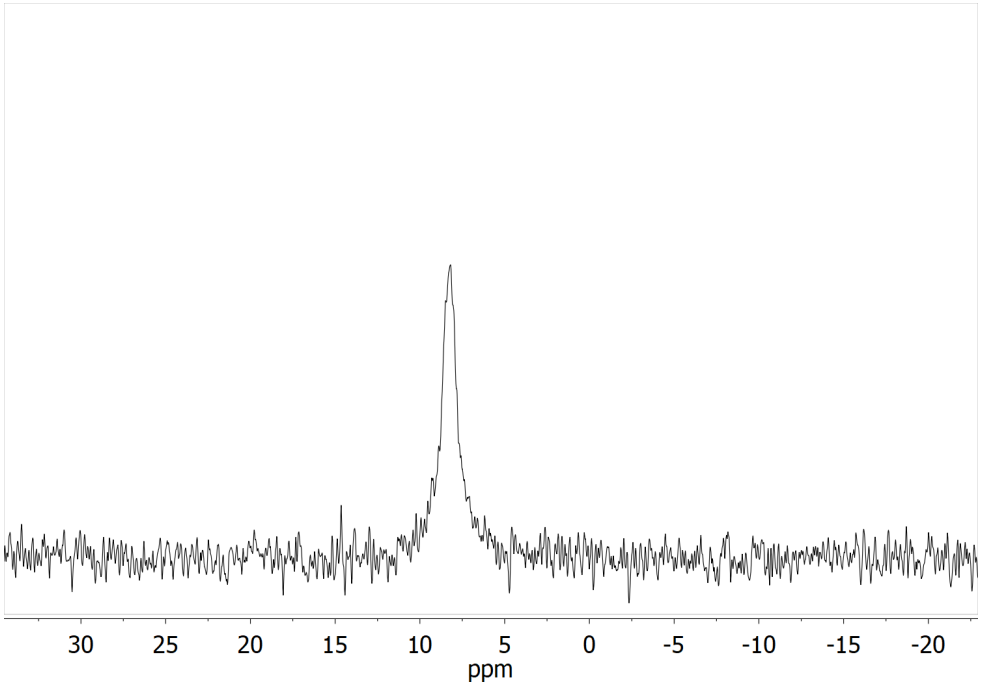

Figure S5. ^{31}P NMR spectrum of complex **1** in an 80/20 mixture of CD_3CN and D_2O.

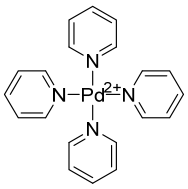

2

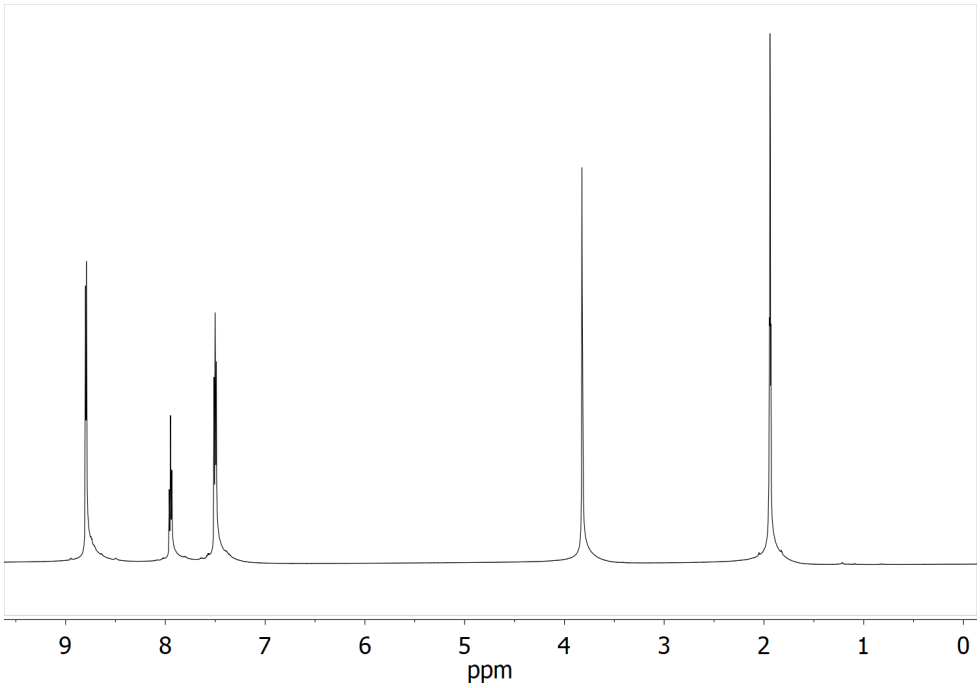

Figure S6. ^{1}H NMR spectrum of complex **2** in an 80/20 mixture of CD_3CN and D_2O.

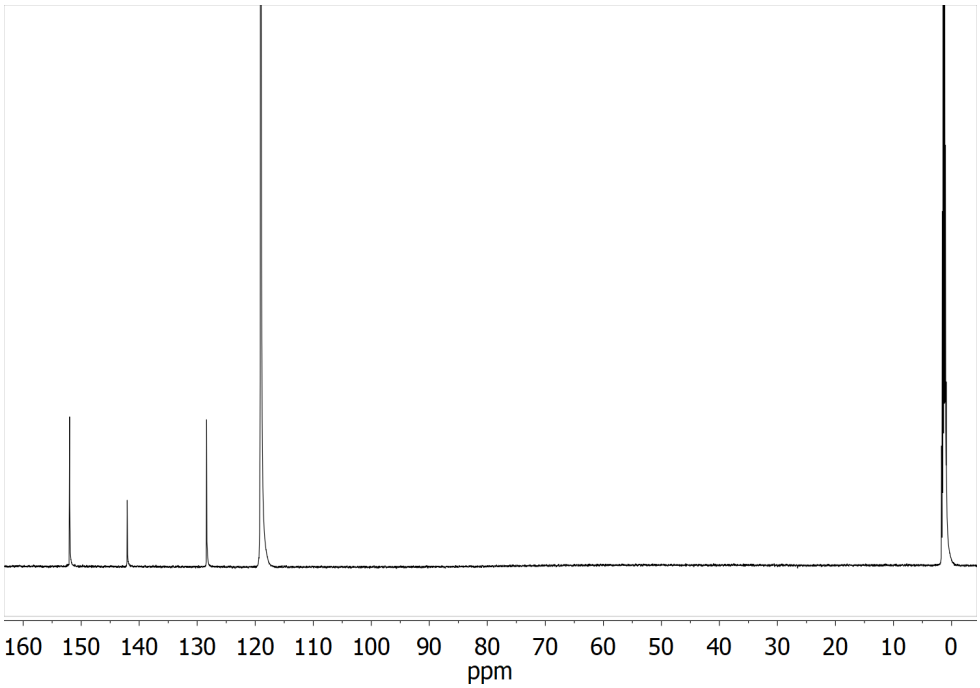

Figure S7. ^{13}C NMR spectrum of complex **2** in an 80/20 mixture of CD_3CN and D_2O.

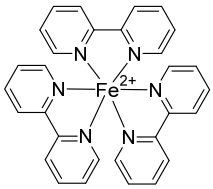

3

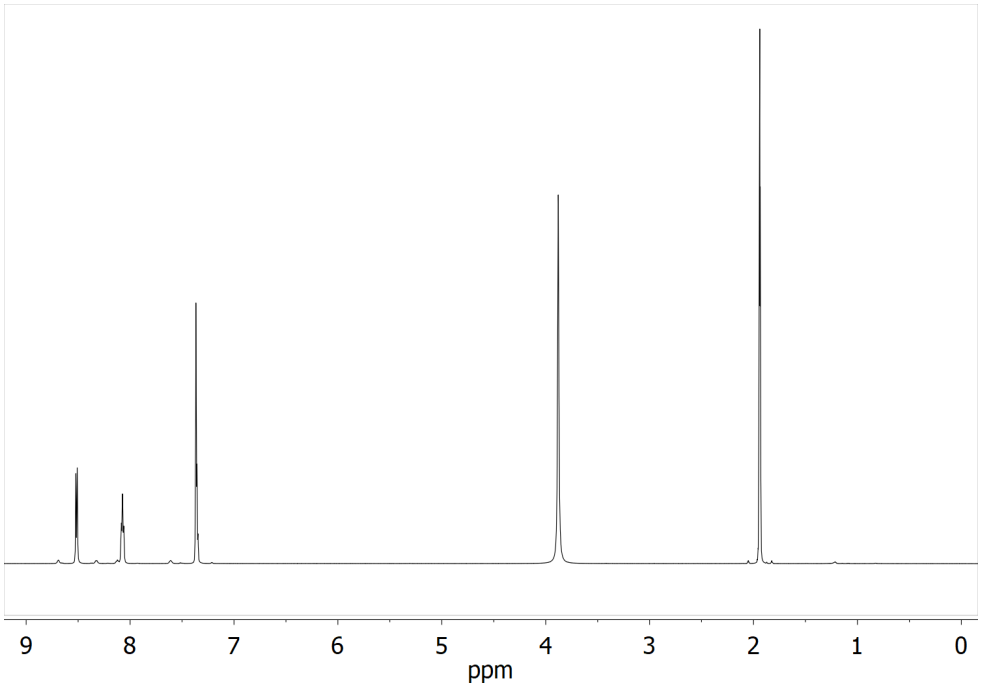

Figure S8. ^{1}H NMR spectrum of complex **3** in an 80/20 mixture of CD_3CN and D_2O.

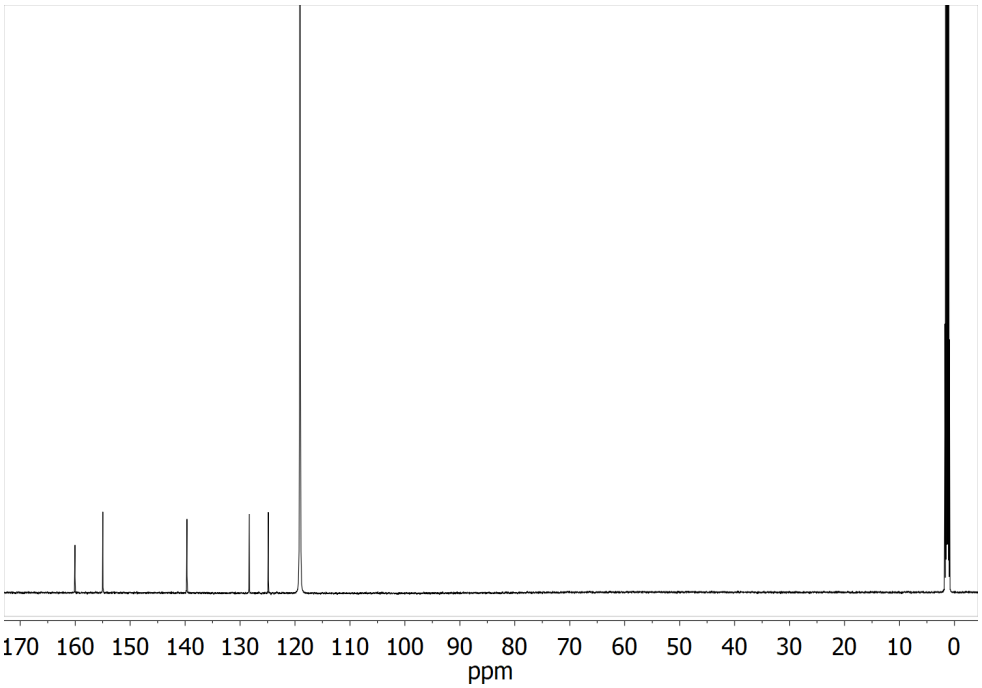

Figure S9. ^{13}C NMR spectrum of complex **3** in an 80/20 mixture of CD_3CN and D_2O.

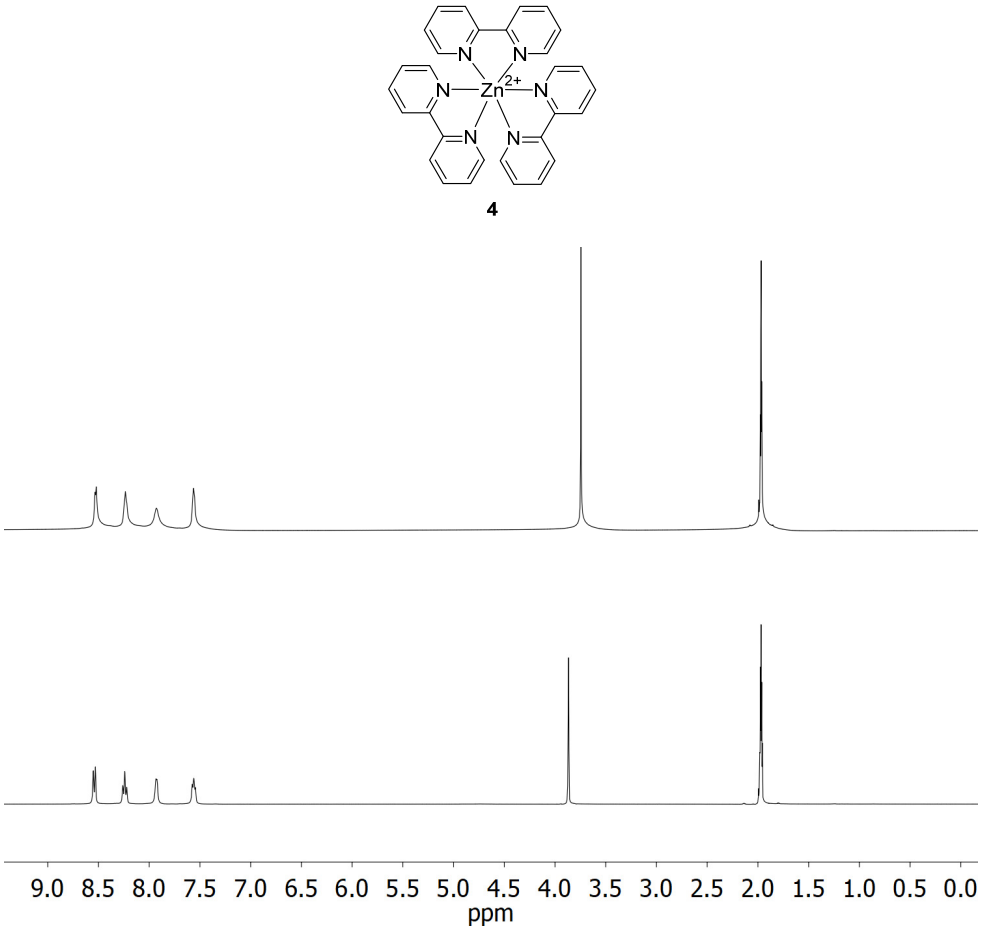

Figure S10. ^{1}H NMR spectrum of complex **4** in an 80/20 mixture of CD_3CN and D_2O at 298K (top) and 275K (bottom).

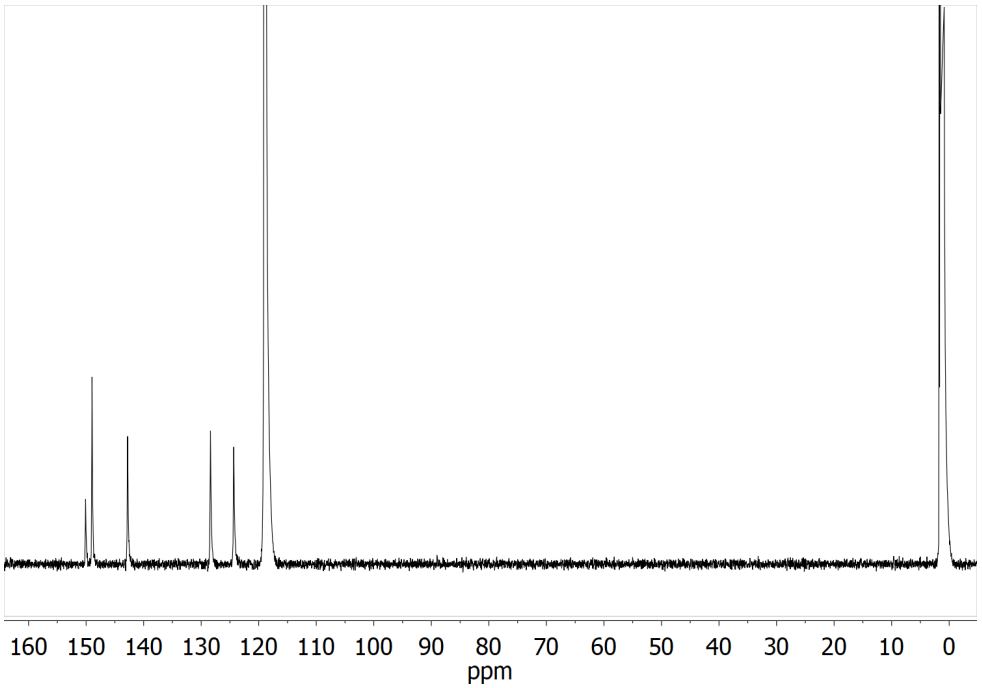

Figure S11. ^{13}C NMR spectrum of complex **4** in an 80/20 mixture of CD_3CN and D_2O.

3.2. Gyrobifastigium 6

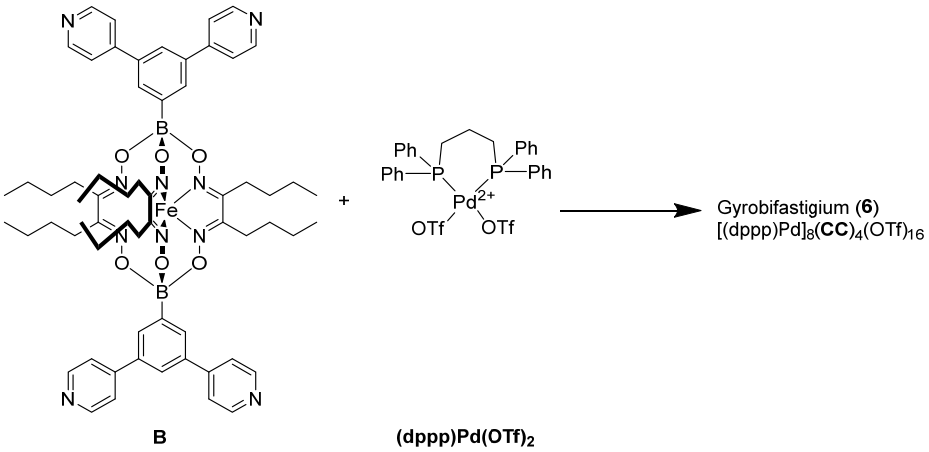

Scheme S1. Synthesis of the gyrobifastigium **6**.

Ligand **B** (12.9 mg, 11.36 μmol) and (dppp)Pd(OTf)$_2$ (19.5 mg, 23.81 μmol) were suspended in degassed CH_3CN (5 mL) and the reaction mixture was stirred for 5 h at 50 °C under N_2. The solution became clear after approximately 20 minutes. The solution was filtered using *Whatman* glass filters. A mixture of Et_2O/pentane (1:5, 60 mL) was added and the flask was transferred placed in a fridge for 20 min. The resulting precipitates were isolated by filtration and dried under vacuum to give the product in the form of an orange powder.

^{1}H NMR (400 MHz, CD_3CN) δ 8.85 – 8.60 (4H), 7.92 – 7.16 (m, 27H), 3.23 (m, 4H), 2.93 – 2.72(m, 1H), 2.58 – 2.34 (m, 6H), 1.64 – 1.40 (m, 1H),1.15 (q, *J* = 14.7, 10.8 Hz, 6H), 0.90 (h, *J* = 6.8 Hz, 6H), 0.31 (t, *J* = 7.3 Hz, 9H). ^{31}P NMR (162 MHz, CD_3CN, referenced on an external standard of 85% H_3PO_4) δ 8.95 (s), 8.90 (s).

Due to the low solubility of this complex, a ^{13}C NMR spectrum was not recorded.

HRMS (ESI): calcd. for $[C_{464}H_{512}B_8Fe_4N_{40}O_{24}P_{16}Pd_8(CF_3SO_3)_{12}]^{4+}$: 2617.5129; found: 2617.5256 and $[C_{464}H_{512}B_8Fe_4N_{40}O_{24}P_{16}Pd_8(CF_3SO_3)_{11}]^{5+}$: 2064.2297; found: 2064.2290.

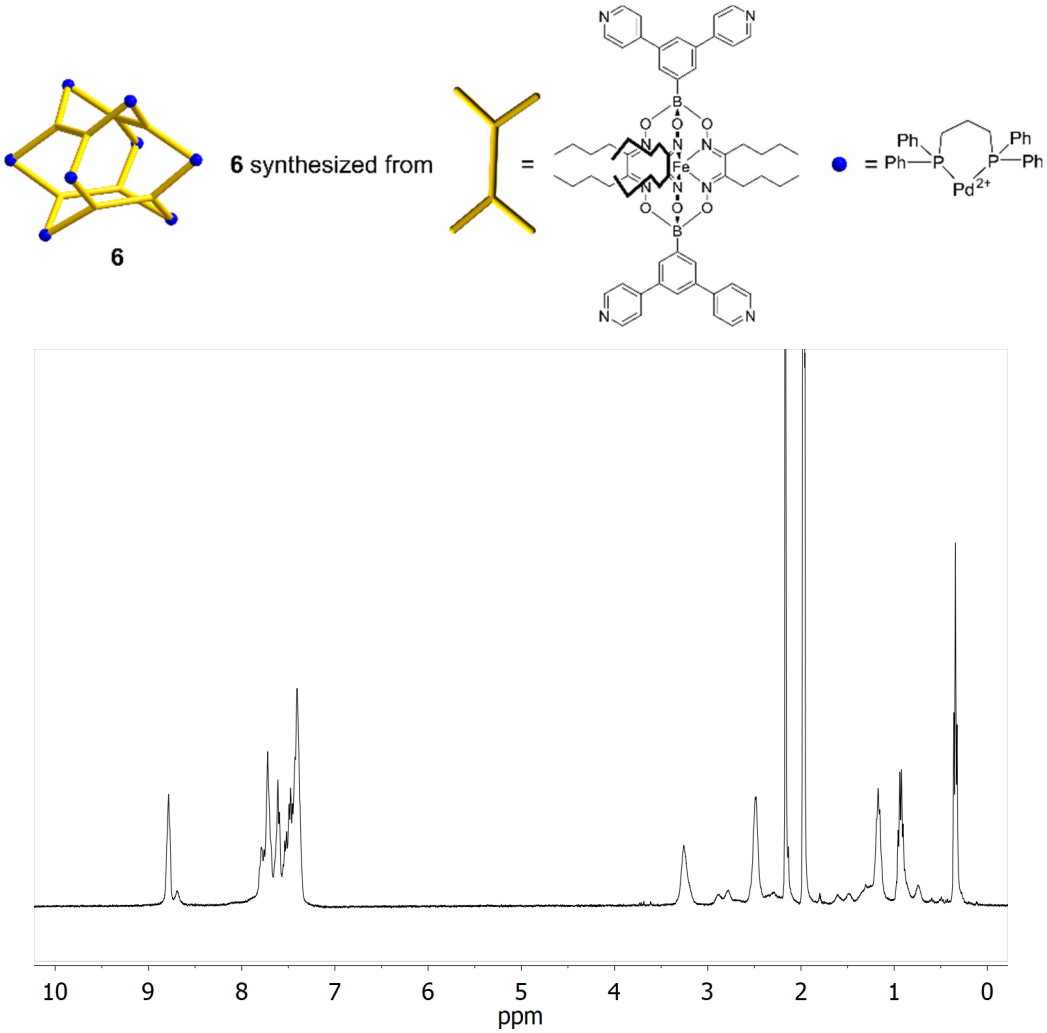

Figure S12. ^{1}H NMR spectrum of gyrobifastigium **6** in CD_3CN. The spectrum suggests the presence of a small amount if a structural isomer.

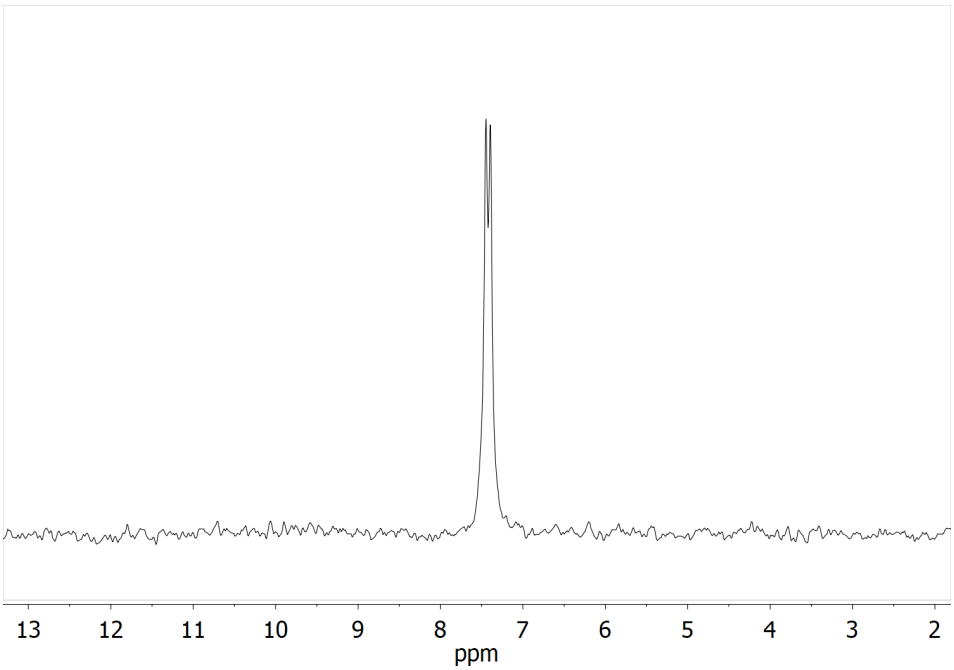

Figure S13. ^{31}P NMR spectrum of gyrobifastigium **6** in CD_3CN with an external standard of 85% H_3PO_4.

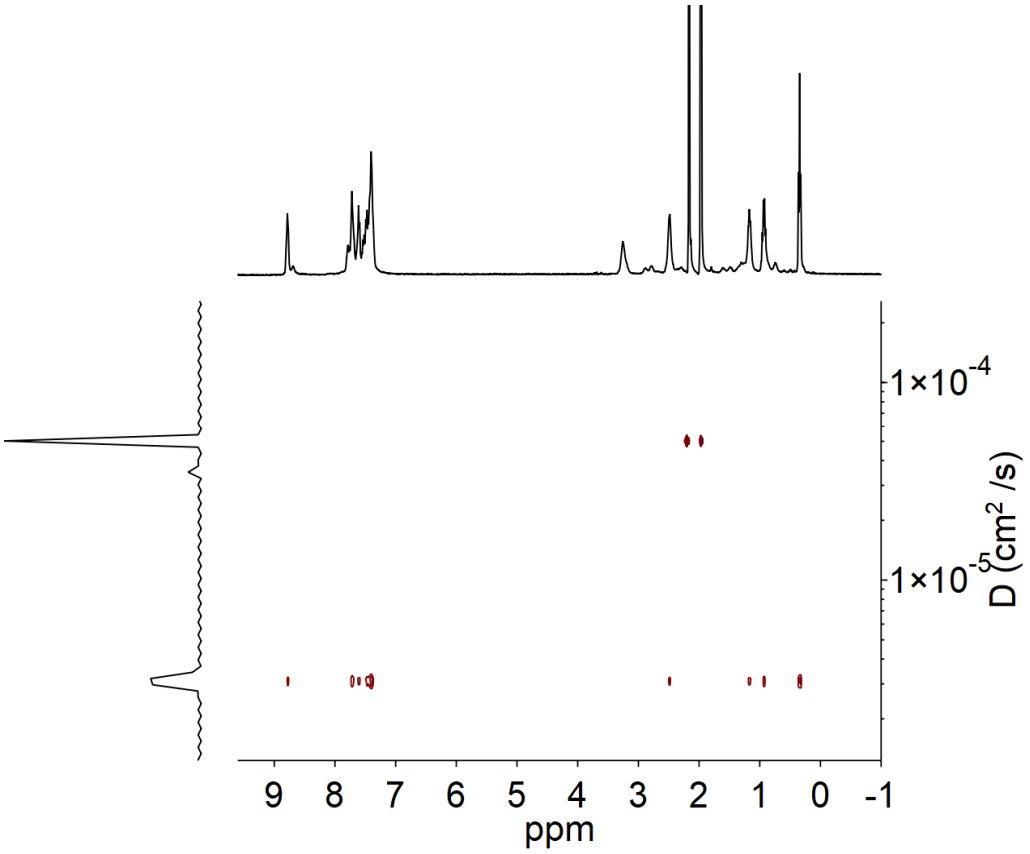

Figure S14. ^{1}H DOSY NMR spectrum of gyrobifastigium **6** in CD_3CN.

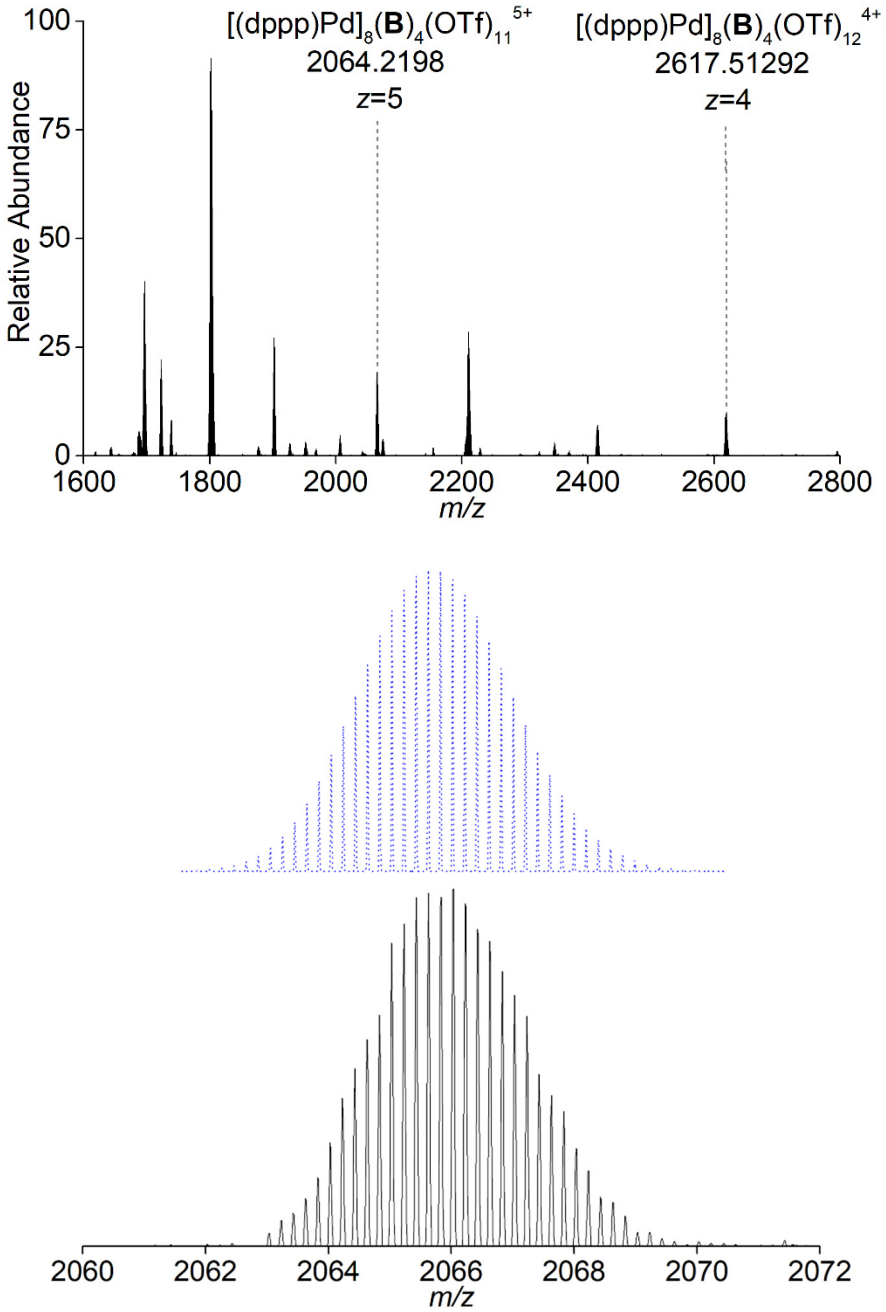

Figure S15. Top: HRMS spectrum of gyrobifastigium **6** in CH_3CN (top). Bottom: Zoom-in of the peak at 2066 *m/z* along with simulated spectrum shown in blue.

4. NMR analyses

NMR spectra of the protonated ligands were obtained from samples containing the ligand and an excess of HCl (pH around 1).

The samples were first measured, then irradiated for 20 minutes (indicated by “light”), then measured again, and left in the dark for 8 hours (indicated by “dark”), followed by a final measurement. Based on the integration of selected signals, the amount of disassembled structure was estimated. When this estimate falls between 80–100 %, it is indicated with >80%.

4.1. Model complexes (1–4)

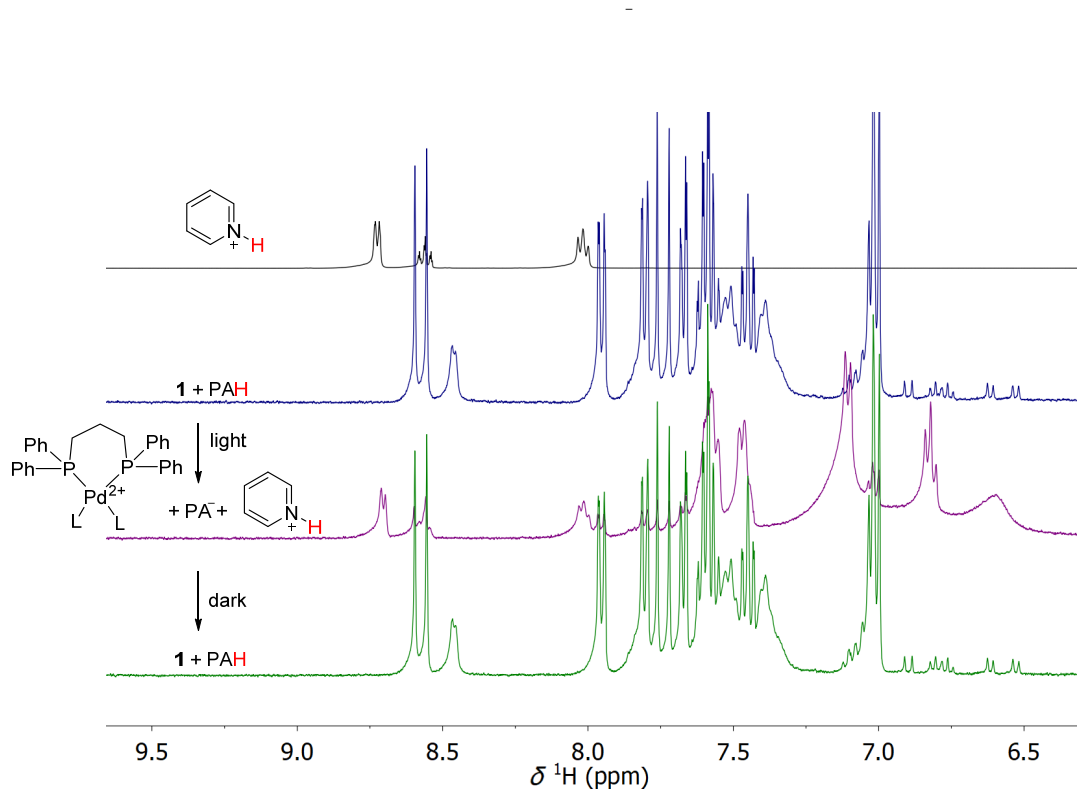

Figure S16. ^{1}H NMR spectrum of protonated pyridine (top) and the photoacid-mediated disassembly of complex **1** in an 80/20 mixture of CD_3CN and D_2O. >80% of the complex disassembled upon light irradiation as estimated by integration of selected signals.

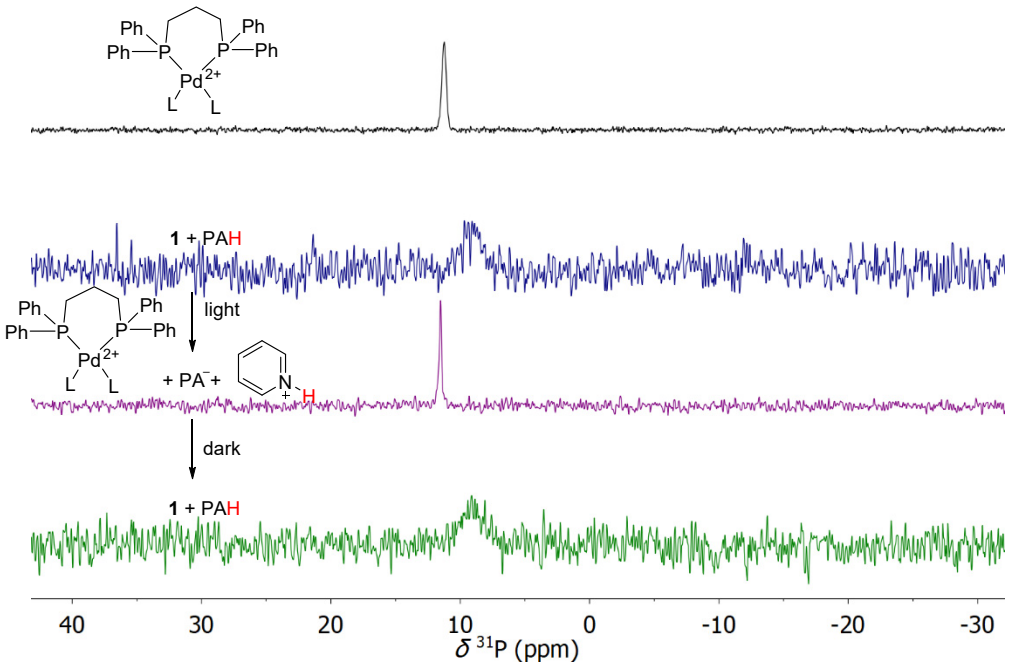

Figure S17. ^{31}P NMR spectrum of [(dppp)Pd(OTf)$_2$] (top) and the photoacid-mediated disassembly of complex **1** in an 80/20 mixture of CD_3CN and D_2O. >80% of the complex disassembled upon light irradiation as estimated by integration of selected signals.

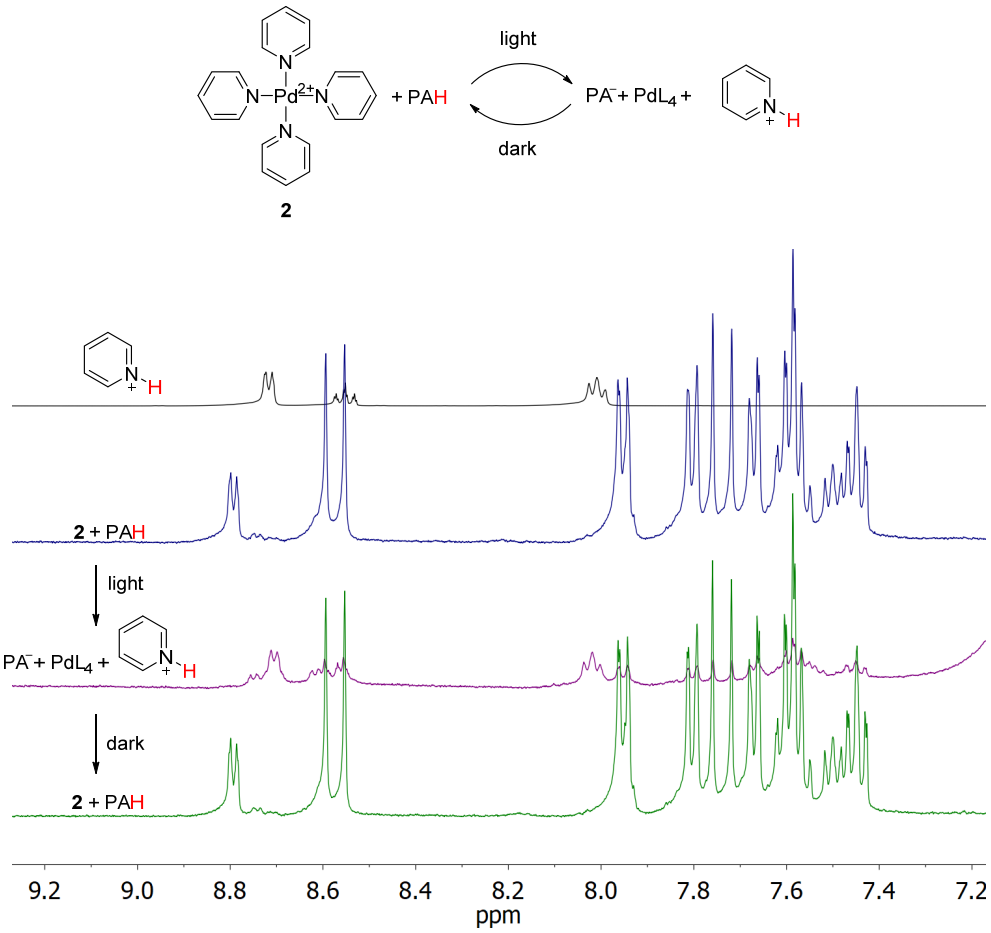

Figure S18. ^{1}H NMR spectrum of protonated pyridine (top) and the photoacid-mediated disassembly of complex **2** in an 80/20 mixture of CD_3CN and D_2O. >80% of the complex disassembled upon light irradiation as estimated by integration of selected signals.

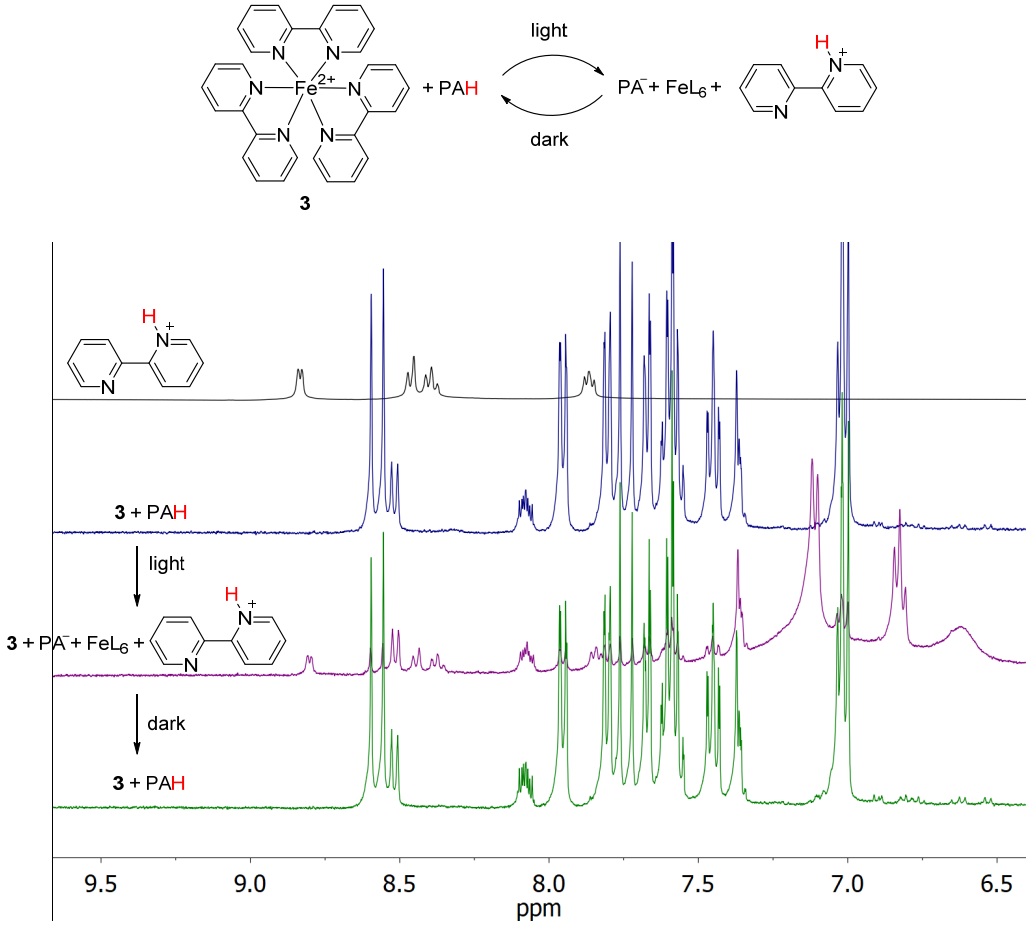

Figure S19. ^{1}H NMR spectrum of protonated 2,2'-bipyridine (top) and the photoacid-mediated disassembly of complex **3** in an 80/20 mixture of CD_3CN and D_2O. 54% of the complex disassembled upon light irradiation as estimated by integration of selected signals.

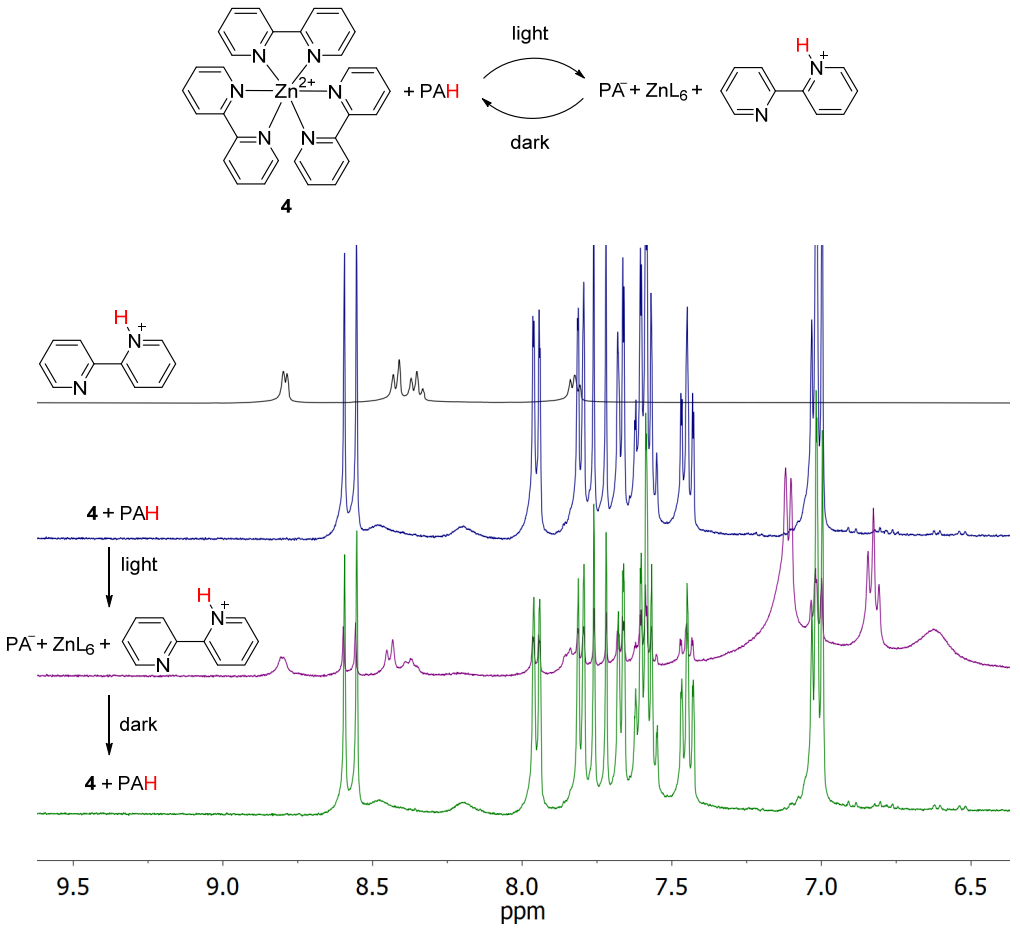

Figure S20. ^{1}H NMR spectrum of protonated 2,2'-bipyridine (top) and the photoacid-mediated disassembly of complex **4** in an 80/20 mixture of CD_3CN and D_2O. >80% of the complex disassembled upon light irradiation as estimated by integration of selected signals.

4.2. Metallasupramolecular structures (5–10)

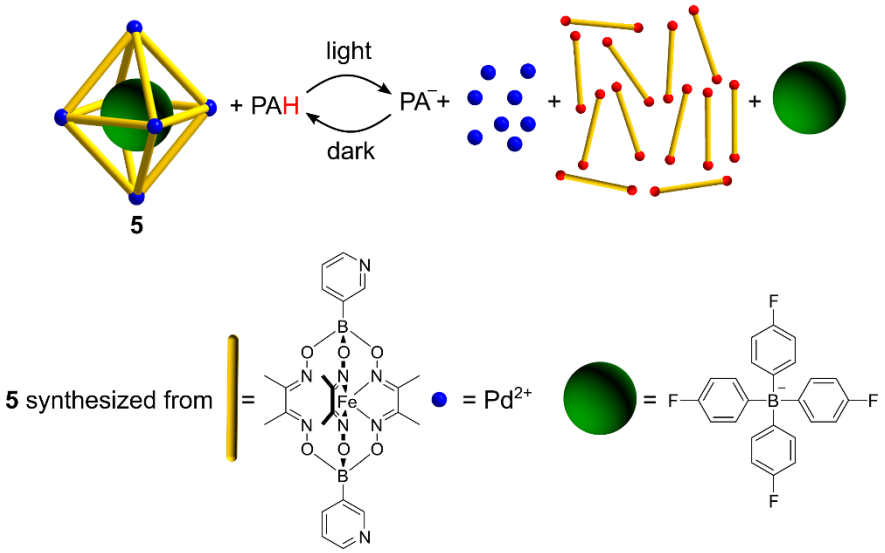

The samples of the octahedron **5** contain 2 equivalents of sodium tetrakis(4-fluorophenyl)borate. To facilitate the disassembly process, 6 equivalents of NaCl were added to the mixture (higher amounts lead to chloride-induced disassembly).

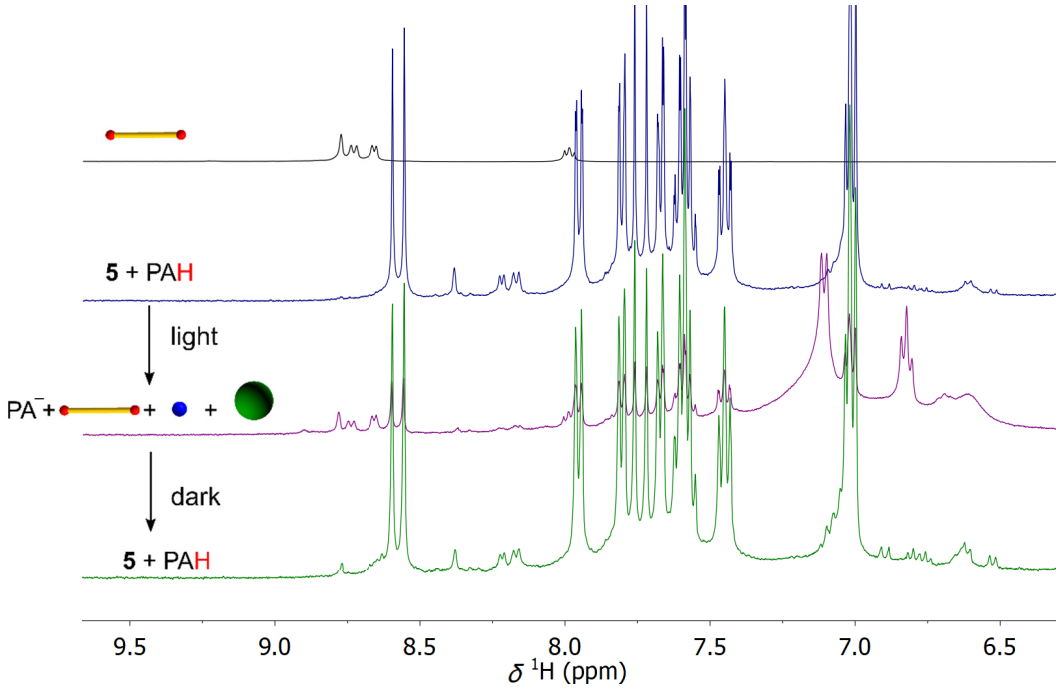

Figure S21. ^{1}H NMR spectrum of the protonated ligand (top) and the photoacid mediated-disassembly of cage **5** in an 80/20 mixture of CD_3CN and D_2O. >80% of the complex disassembled upon light irradiation as estimated by integration of selected signals.

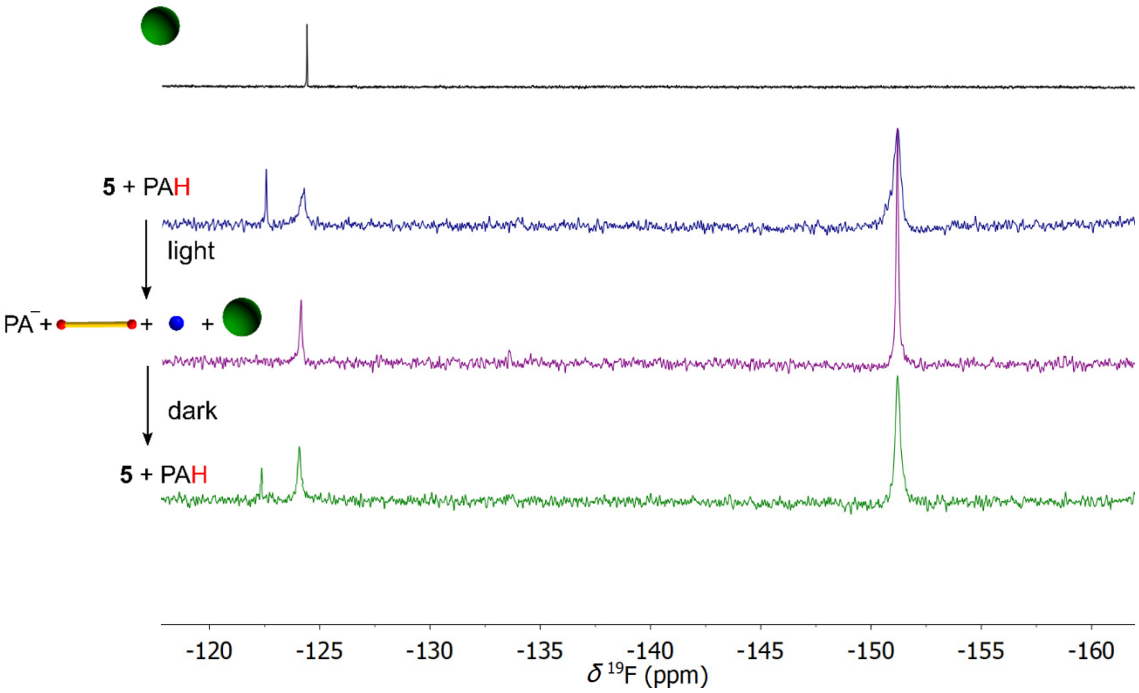

Figure S22. ^{19}F NMR spectrum of guest (top) and the photoacid-mediated disassembly of cage **5** in an 80/20 mixture of CD_3CN and D_2O. >80% of the complex disassembled upon light irradiation as estimated by integration of selected signals.

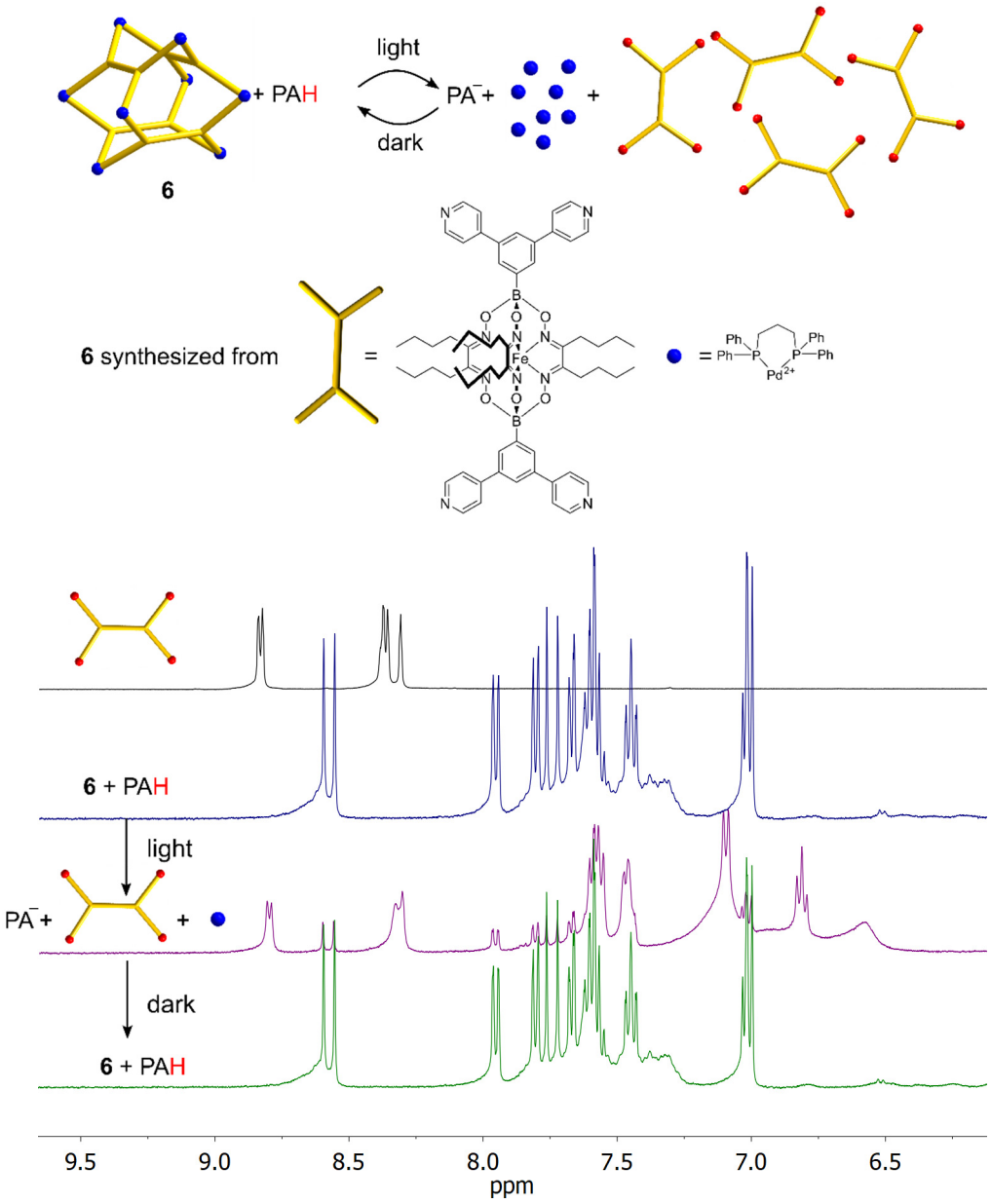

Figure S23. ^{1}H NMR spectrum of the protonated ligand (top) and the photoacid-mediated disassembly of cage **6** in an 80/20 mixture of CD_3CN and D_2O. >80% of the complex disassembled upon light irradiation as estimated by integration of selected signals.

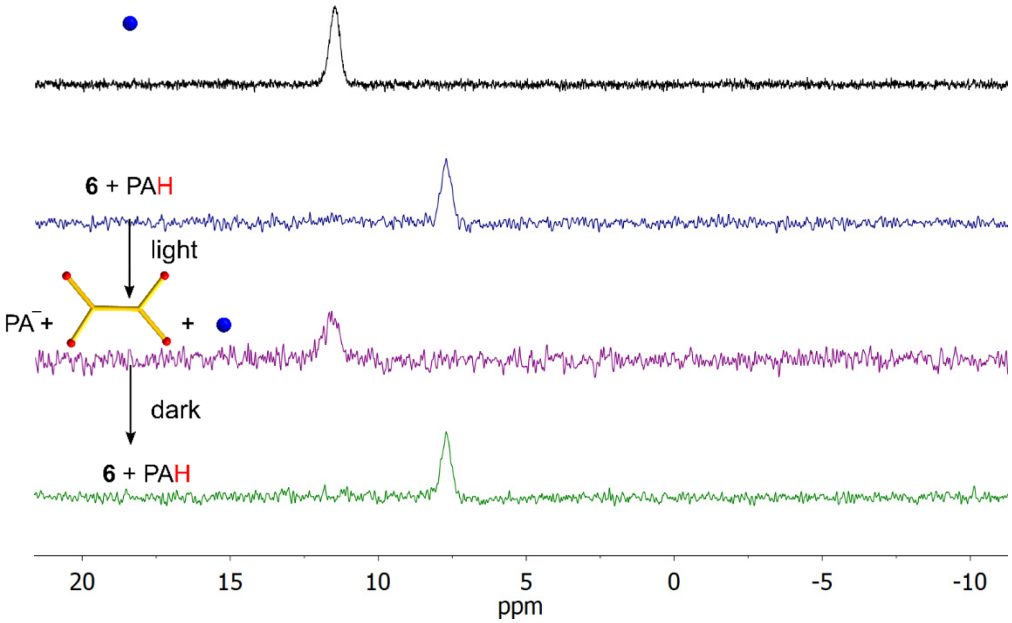

Figure S24. ^{31}P NMR spectrum of [(dppp)Pd(OTf)$_2$] (top) and the photoacid-mediated disassembly of cage **6** in an 80/20 mixture of CD_3CN and D_2O. >80% of the complex disassembled upon light irradiation as estimated by integration of selected signals.

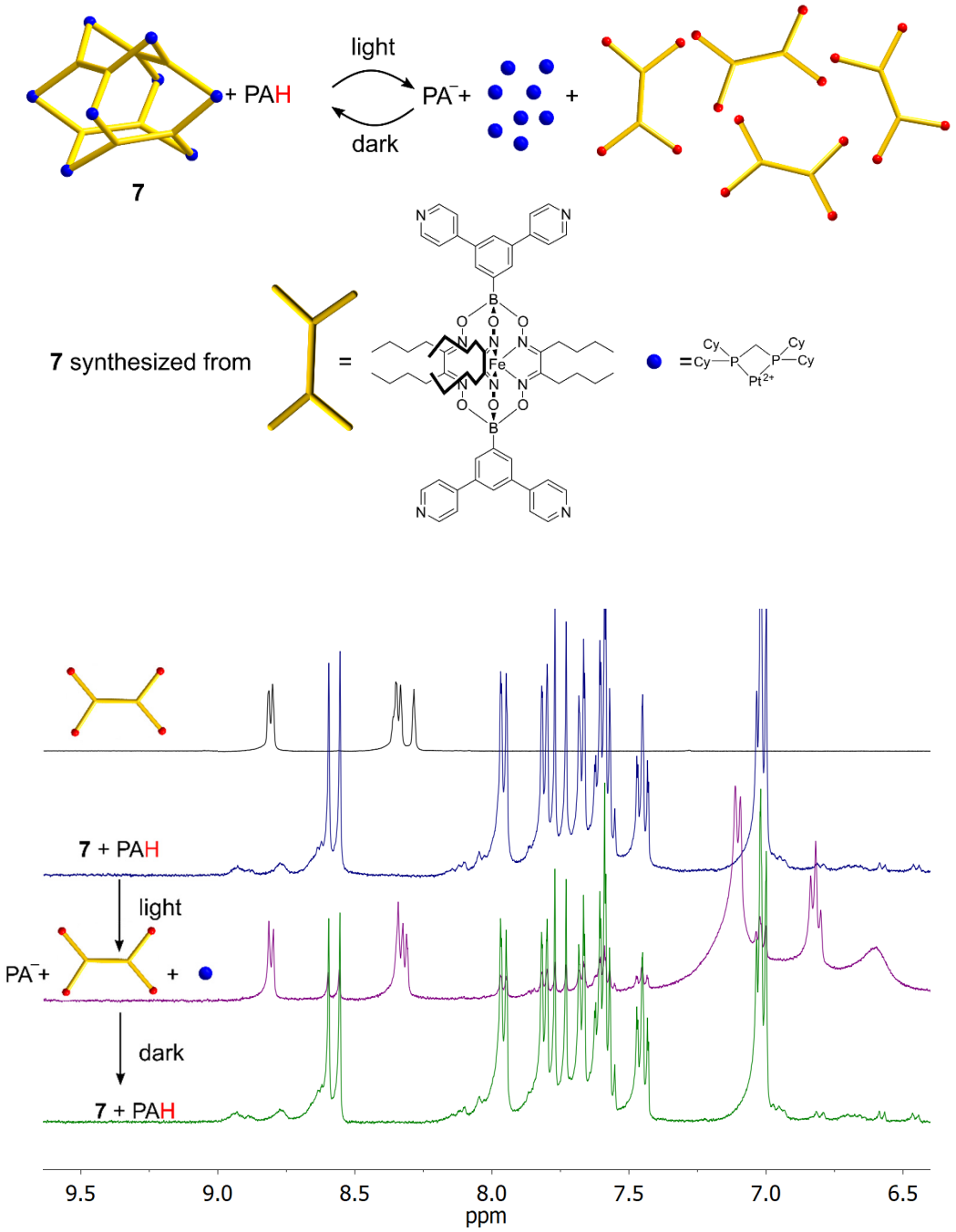

Figure S25. ^{1}H NMR spectrum of the protonated ligand (top) and the photoacid-mediated disassembly of cage **7** in an 80/20 mixture of CD_3CN and D_2O. >80% of the complex disassembled upon light irradiation as estimated by integration of selected signals.

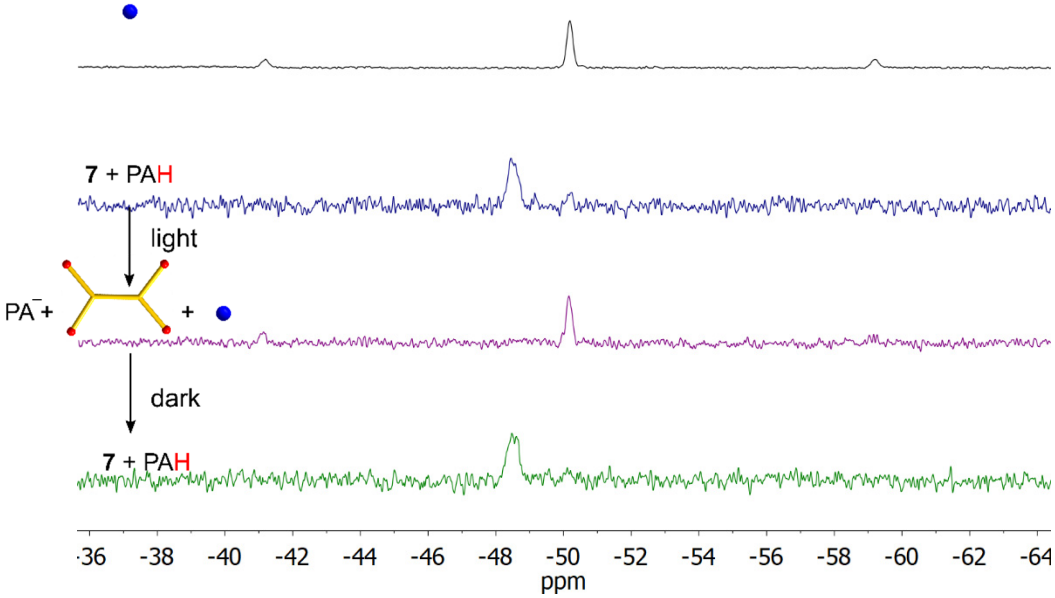

Figure S26. ^{31}P NMR spectrum of [(dcpm)Pt(OTf)$_2$] (top) and the photoacid-mediated disassembly of cage **7** in an 80/20 mixture of CD_3CN and D_2O. >80% of the complex disassembled upon light irradiation as estimated by integration of selected signals.

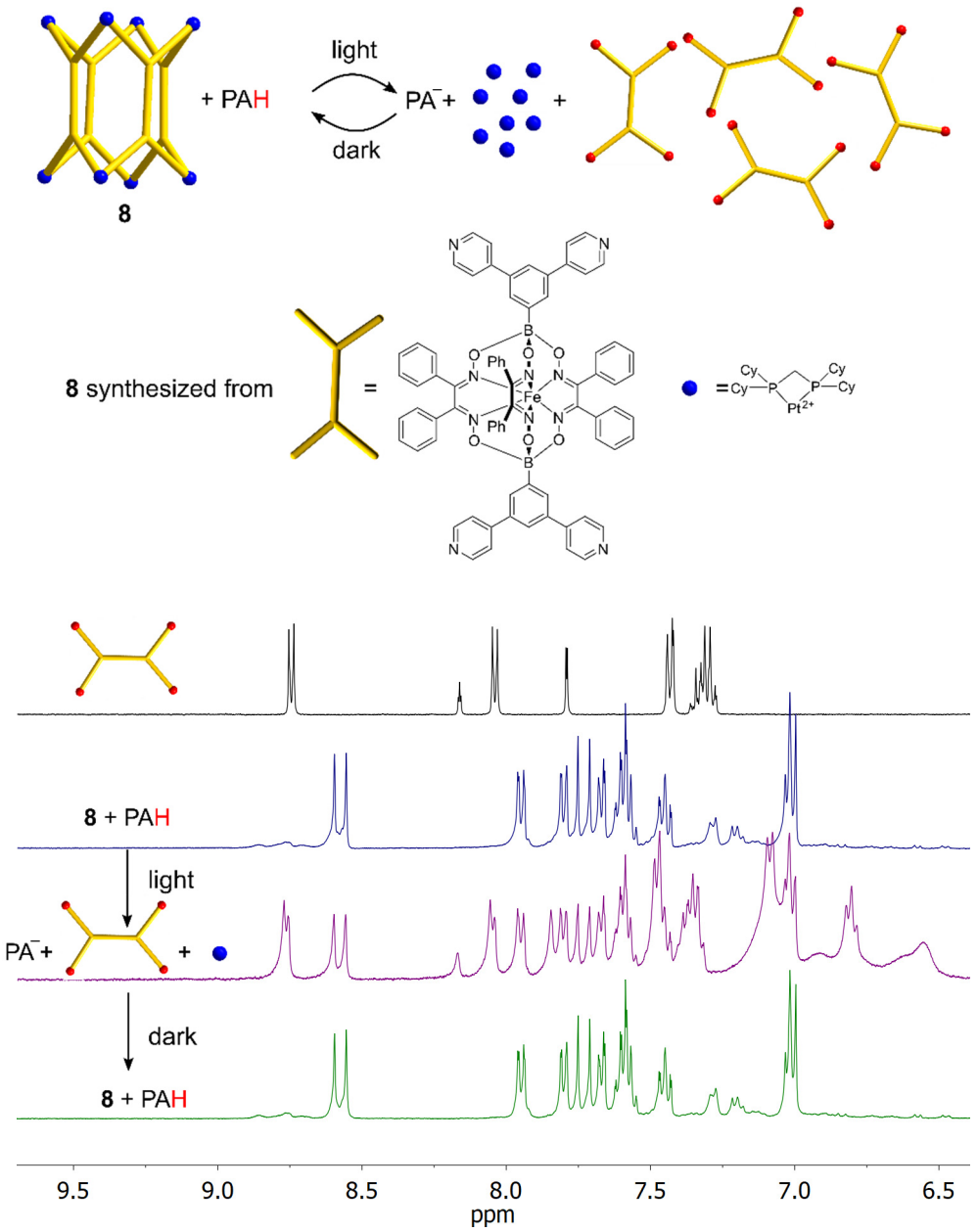

Figure S27. ^{1}H NMR spectrum of the protonated ligand (top) and the photoacid-mediated disassembly of cage **8** in an 80/20 mixture of CD_3CN and D_2O. >80% of the complex disassembled upon light irradiation as estimated by integration of selected signals.

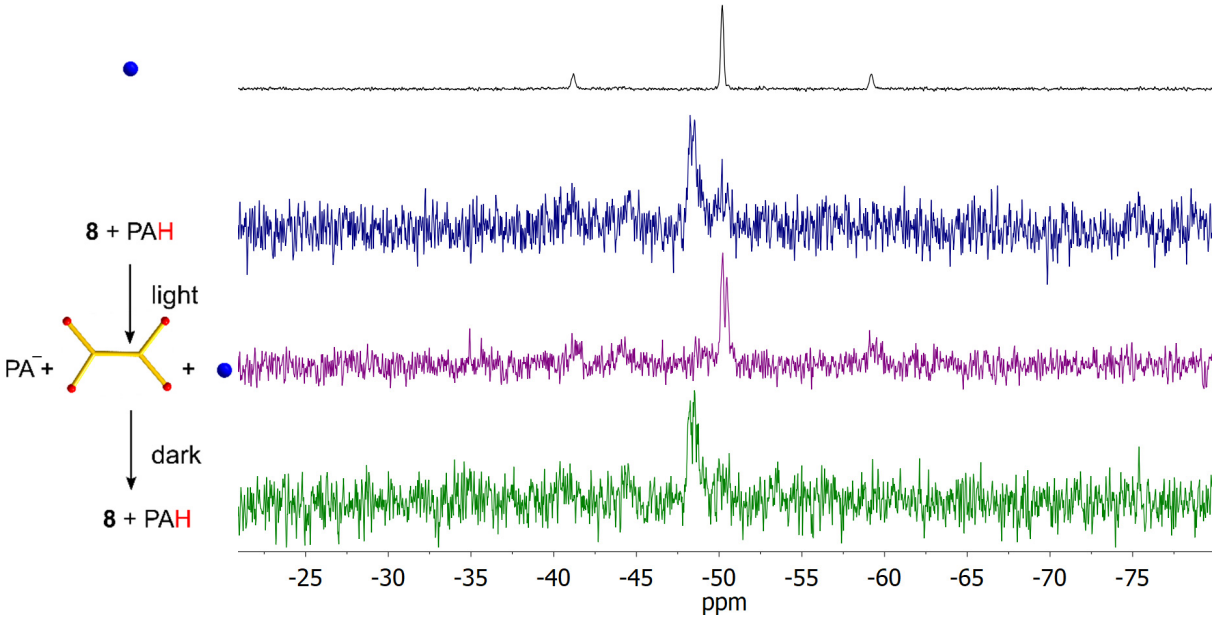

Figure S28. ^{31}P NMR spectrum of [(dcpm)Pt(OTf)$_2$] (top) and the photoacid-mediated disassembly of cage **8** in an 80/20 mixture of CD_3CN and D_2O. >80% of the complex disassembled upon light irradiation as estimated by integration of selected signals.

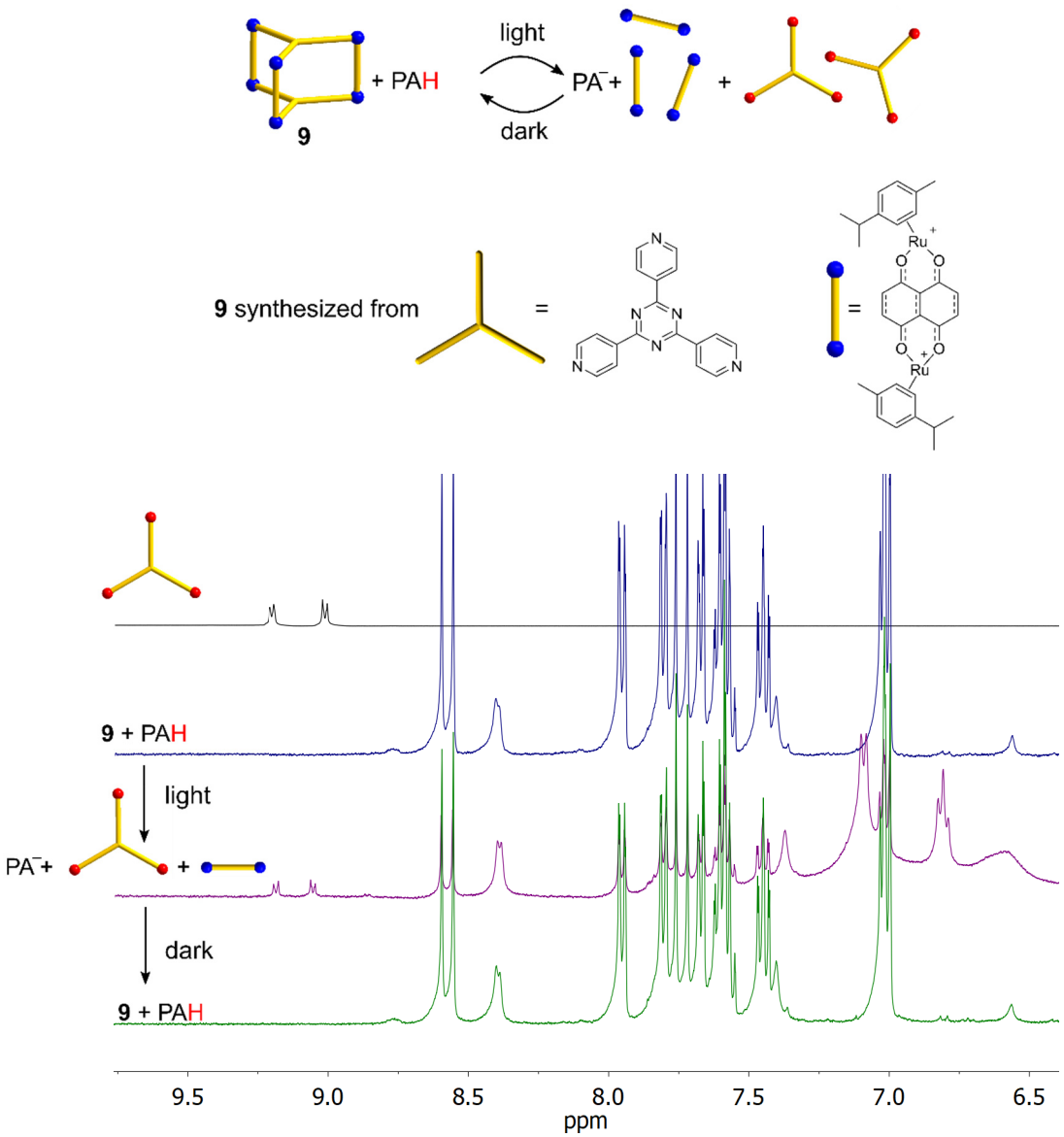

Figure S29. ^{1}H NMR spectrum of the protonated ligand (top) and the photoacid-mediated disassembly of cage **9** in an 80/20 mixture of CD_3CN and D_2O. 16% of the complex disassembled upon light irradiation as estimated by integration of selected signals.

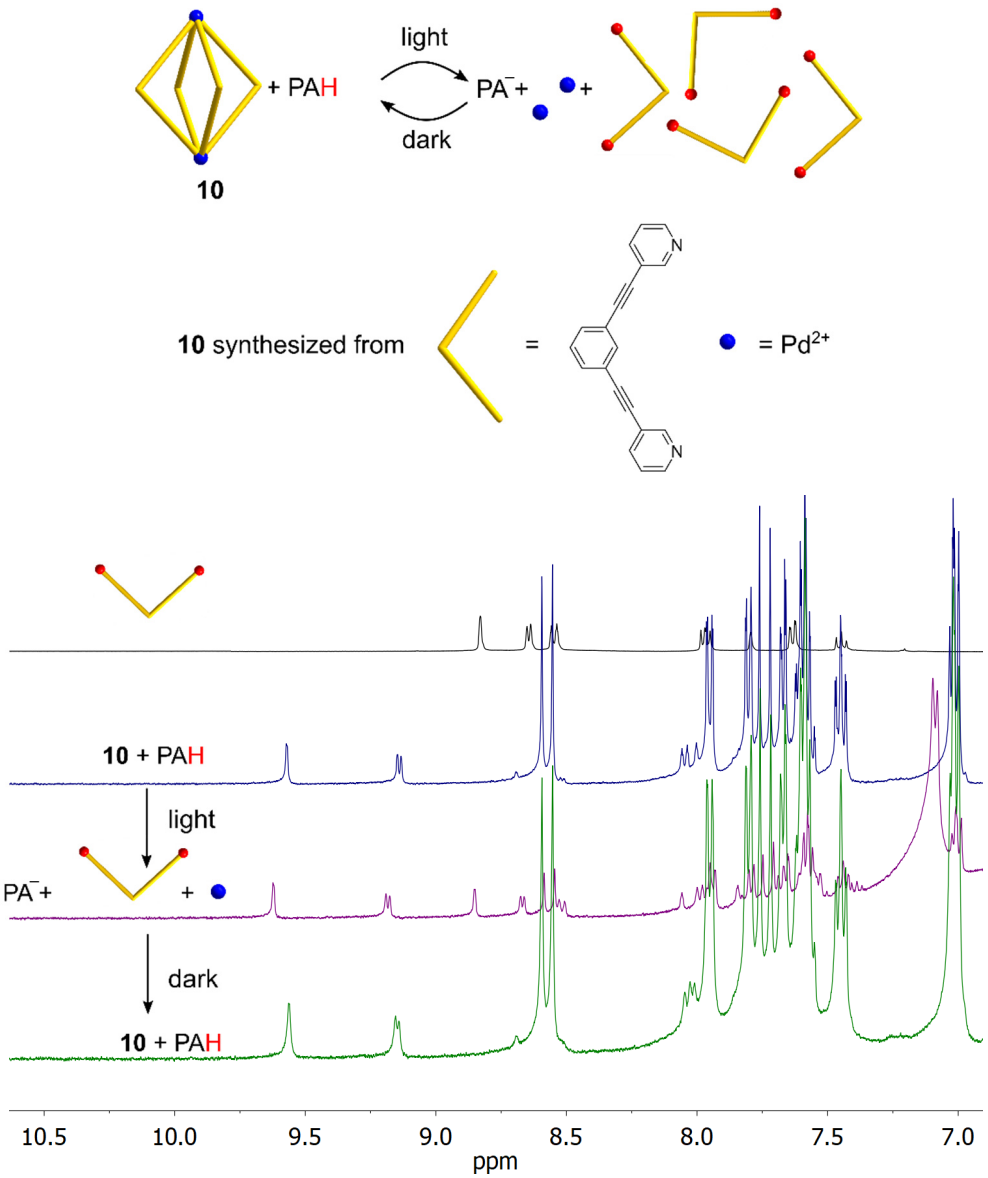

Figure S30. ^{1}H NMR spectrum of the protonated ligand (top) and the photoacid-mediated disassembly of cage **10** in an 80/20 mixture of CD_3CN and D_2O. 45% of the complex disassembled upon light irradiation as estimated by integration of selected signals.

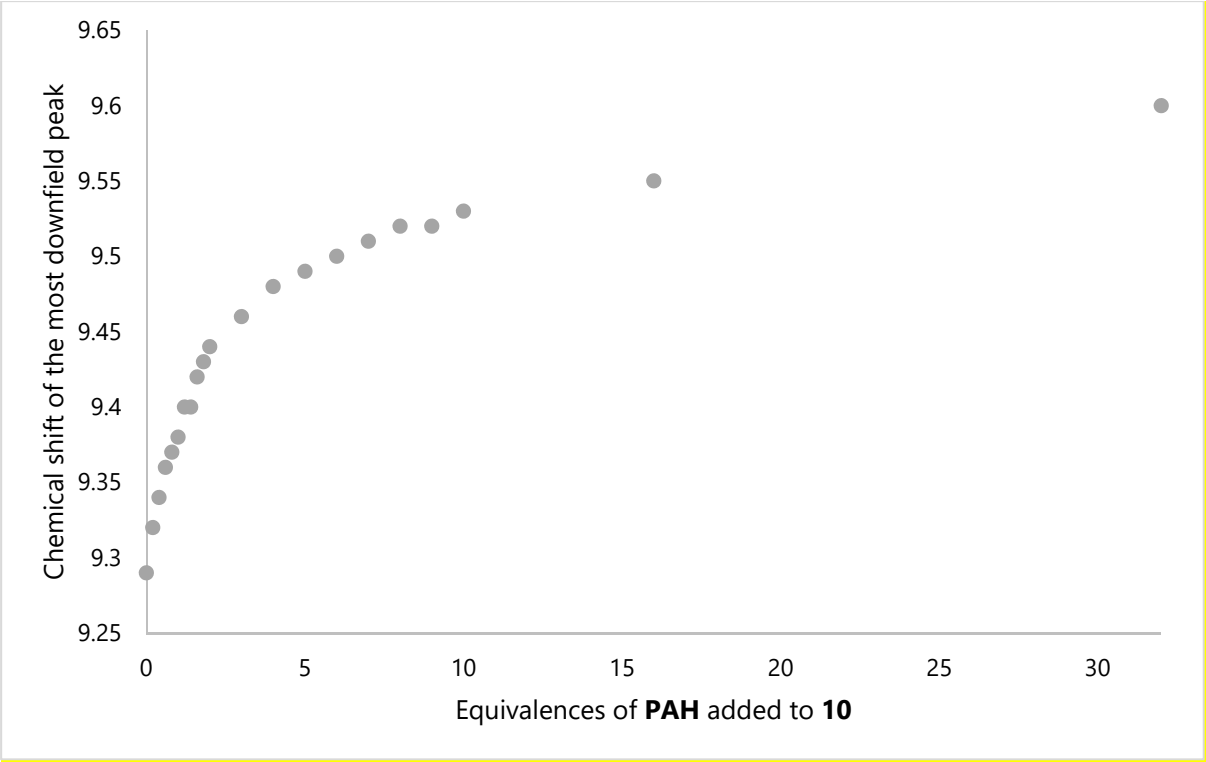

Figure S31. Difference in the chemical shift of a proton NMR signal of cage **10** upon addition of increasing amounts of the photoacid **PAH**. The binding isotherm indicates weak complexation of the photoacid to the cage, presumably via the sulfonate group. The NMR titration was performed as described below.

Experimental details: A solution of cage **10** (1.6 µmol) in an 80/20 mixture of CD_3CN and D_2O (V_{total} = 0.5 mL) was employed. Aliquots (20 µL) of a stock solution of **PAH** in the same solvent mixture (0.32 µmol per 20 µL) were added until 2 equivalences of **PAH** were reached. After each addition, an NMR spectrum was recorded. For subsequent measurements (2–10 equiv. **PAH**), a more concentrated stock solution of **PAH** (1.6 µmol per 10 µL) was employed, and the aliquot volume was reduced to 10 µL. For the last two data points (16 and 32 equiv.), the corresponding amount of **PAH** was added as a solid to the sample (0.4 and 1 mg, respectively). The sample was kept in the dark at all time.

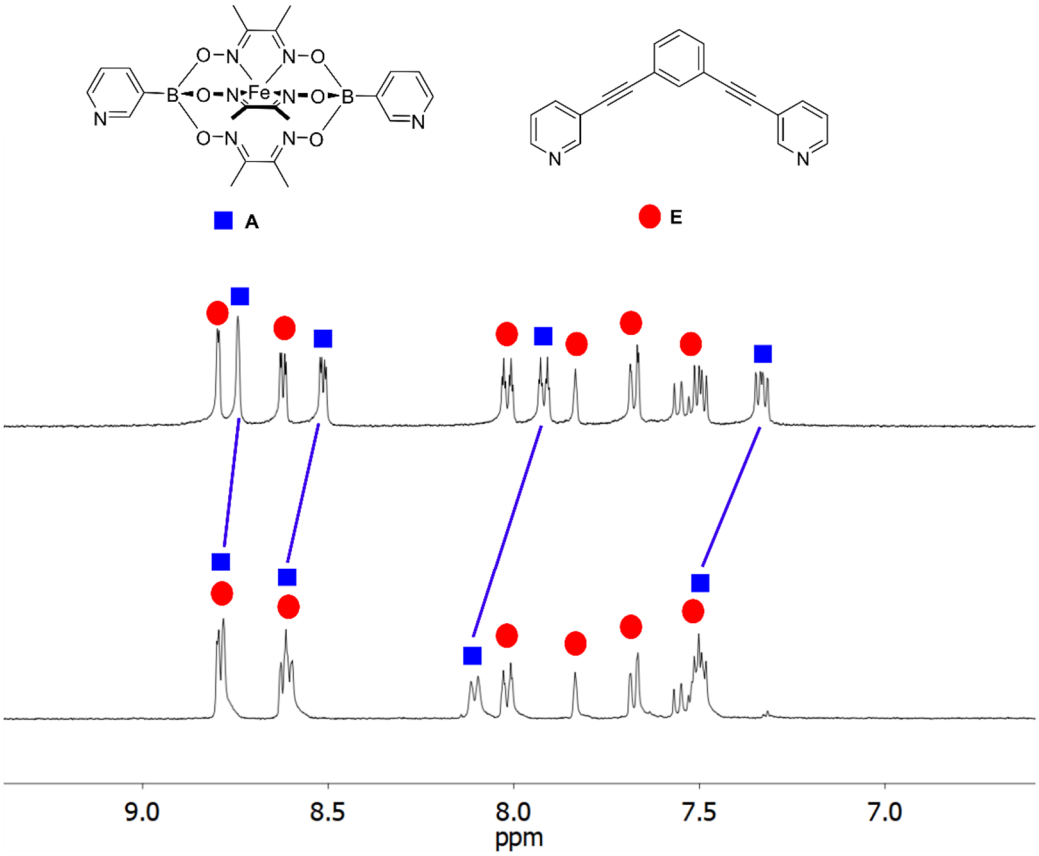

Figure S32. Aromatic part of the ^{1}H NMR spectrum of an equimolar mixture of the ligands **A** and **E** in DMSO-*d6* (top), and a spectrum of the same mixture after addition of 1 equivalent of TFA (bottom). Only the signals of ligand **A** (blue) shift, indicating preferential protonation of **A** over **E**.

Experimental details: A solution of **A** (0.9 mg, 1.6 µmol) and **E** (0.5 mg, 1.6 µmol) was prepared in DMSO-*d6* (1 mL). This sample was divided over two NMR tubes. To one of the tubes, 5 µL of a 3.2 mM stock solution of TFA in a mixture of CD_3CN and D_2O was added.

5. Activation of the photoacid

The behaviour of the photoacid in an 80/20 mixture of CH_3CN and H_2O, was studied by UV-VIS. After obtaining a full UV-VIS spectrum in the dark and after 20 minutes light irradiation, the sample was irradiated again for 20 minutes, and then the absorption between 400 and 460 nm was measured every 12 seconds.

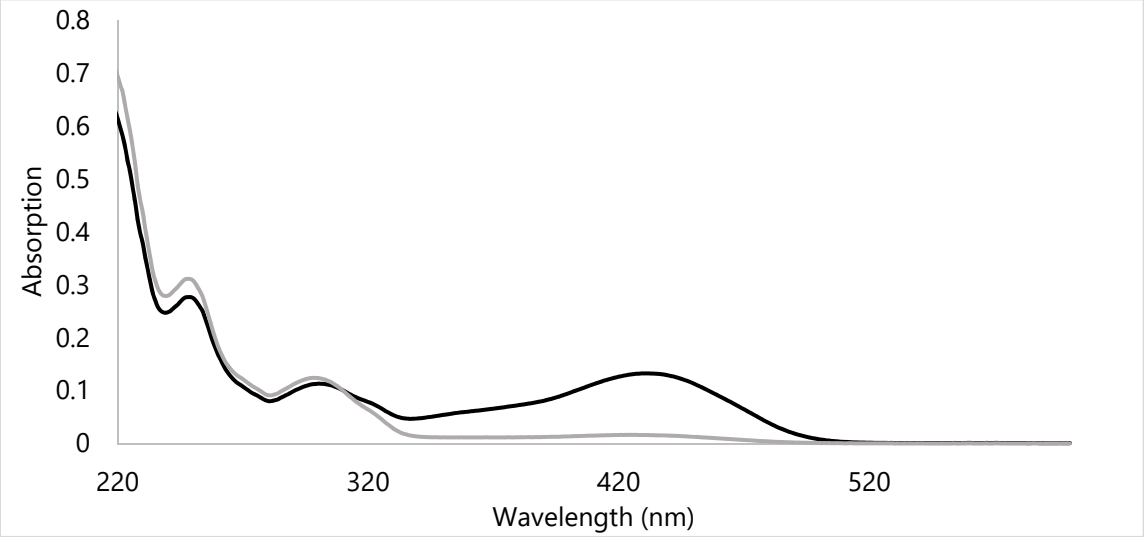

Figure S33. UV-VIS spectra of the photoacid in an 80/20 mixture of CH_3CN and H_2O before (black line) and after (grey line) irradiation.

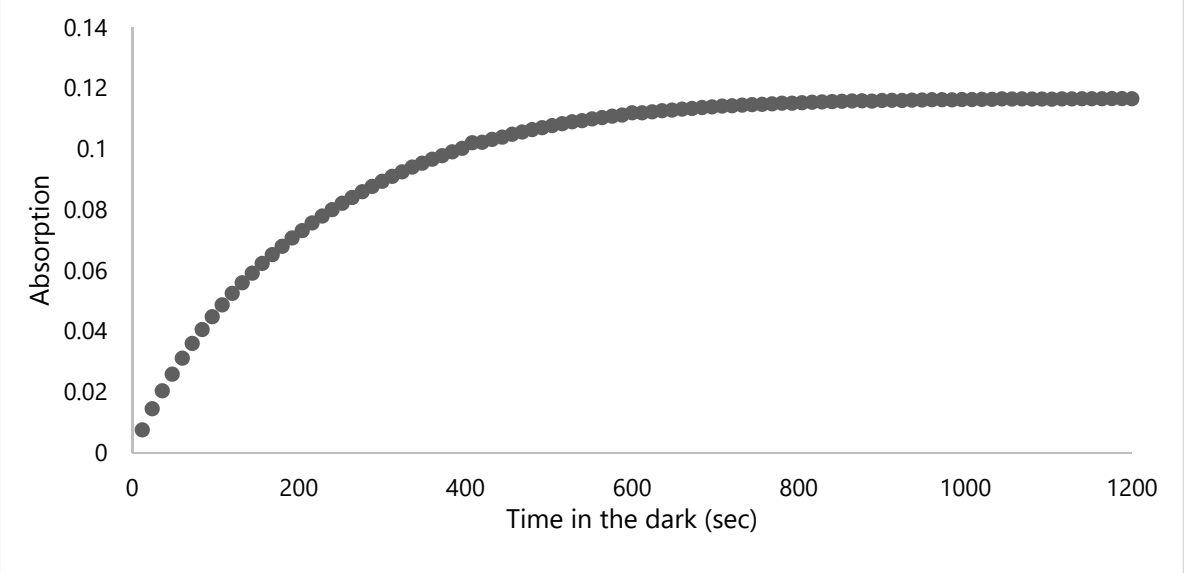

Figure S34. Absorption at 431 nm as a function of time. The photoacid switches back to the non-acidic merocyanine form with a half-life of $t_{1/2}$ = 2.4 minutes.

6. Repetitive disassembly of barrel 8

The coordination barrel **8** was disassembled and re-assembled over 5 cycles. One cycle consists of 20 min light exposure, followed by 2.5 h in the dark. The sample contained DCM as an internal standard, and the change in integration of three separate signals of the protonated ligand **8b** were monitored (average values were used for the data shown in Figure S33/Figure 2).

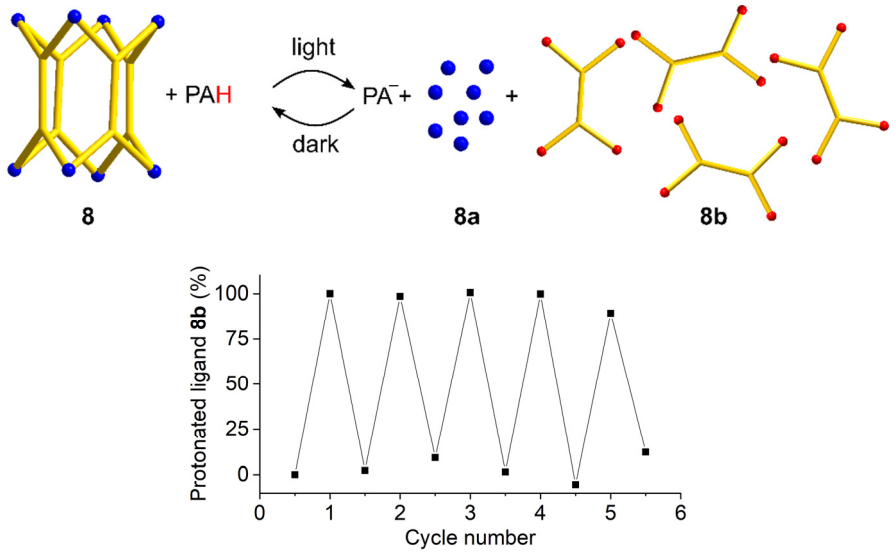

Figure S35. Repeated photo-switching between the coordination barrel **8** and its disassembled state. The relative amount of the protonated ligand **8b** was used as an indication of the switching efficiency. For cycle one, the amount of **8b** was normalized to 0 and 100%, respectively.

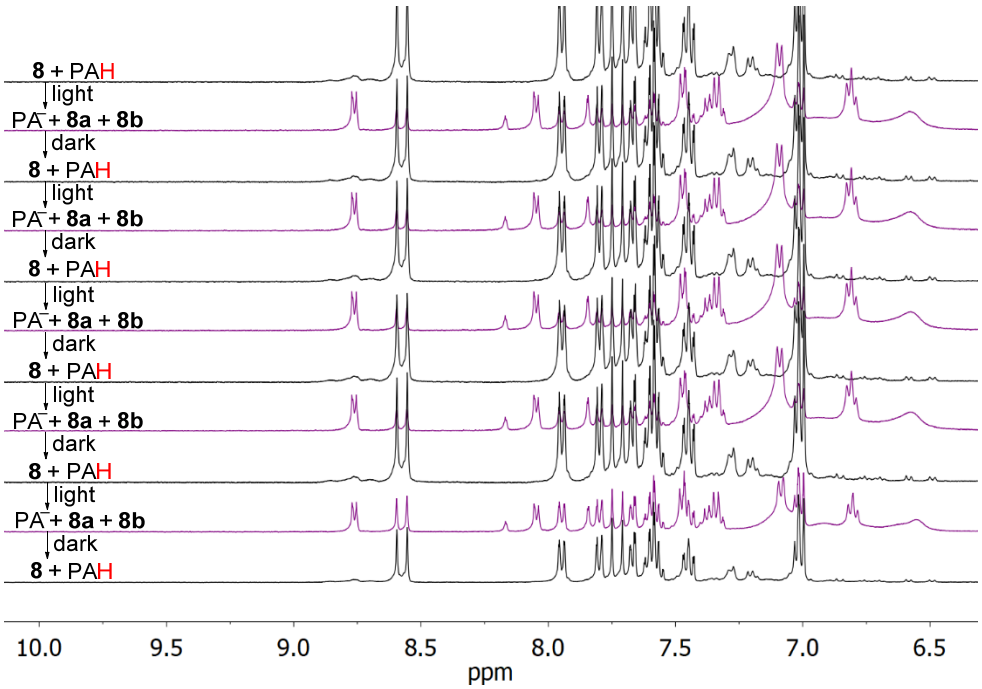

Figure S36. ^{1}H NMR spectra of the repeated photo-switching between the coordination barrel **8** and its disassembled state in an 80/20 mixture of CD_3CN and D_2O.

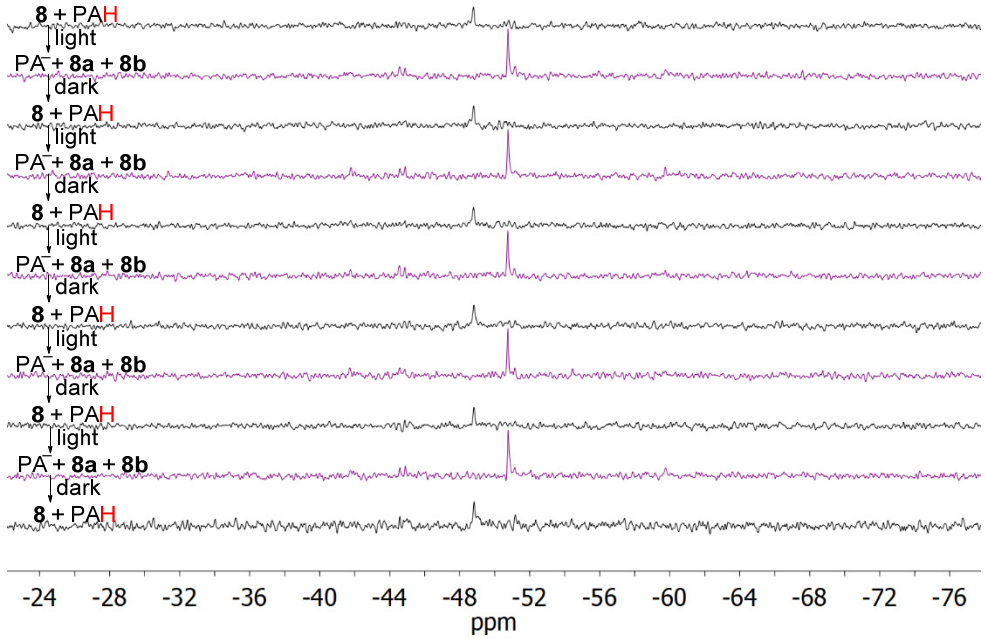

Figure S37. ^{13}P NMR spectra of the repeated photo-switching between the coordination barrel **8** and its disassembled state in an 80/20 mixture of CD_3CN and D_2O.

7. Kinetic study of the re-assembly processes

Samples containing the photoacid and the respective metal complex were irradiated for 20 minutes. ^{1}H NMR spectra were then recorded after 0, 10, 20, and 30 min (for t = 0 the amount of protonated ligand was normalized to 100%). All measurements were performed at 298 K. The signals of the protonated ligand were integrated (DCM was used as internal standard) to give the data depicted below. The amount of the protonated ligand is expected to be indirectly proportional to the amount of re-assembled metal complex. A direct integration of the signals of the supramolecular complexes was hampered by signal overlap with the signals of the photoacid.

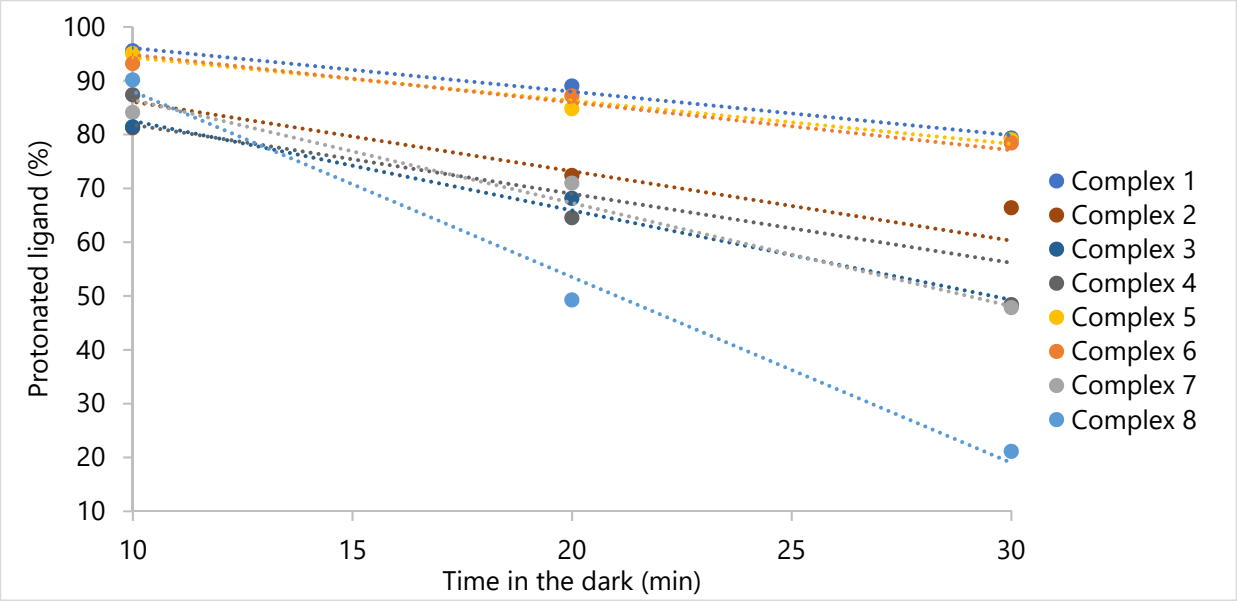

Figure S38. The amount of protonated ligand as a function of time for complexes **1**–**8** in an 80/20 mixture of CD_3CN and D_2O after 10, 20 and 30 minutes in the dark.

Table S2. Estimated half-lifes at 298 K for the re-assembly of the complexes **1**–**8**.

Complex	$t_{1/2}$ (min)
1	67
2	38
3	35
4	30
5	65
6	60
7	29
8	21

For comparison, the reassembly of the complexes **5** and **8** was investigated at 50 °C. For complex **5**, complete reassembly was observed after 30 minutes at 50 °C versus 100 minutes at r.t.. For complex **8**, complete reassembly was observed after 10 minutes at 50 °C versus 30 minutes at r.t..

8. Absorption spectra of the complexes 5, 8 and 9

The visible light absorption of a two selected coordination cages were measured to demonstrate that even though the cages might absorb at a similar wavelength as the photoacid, this does not inhibit the photoswitching behaviour of the mixtures. The absorption spectra were measured in 80/20 acetonitrile/water and they are baseline and blank corrected.

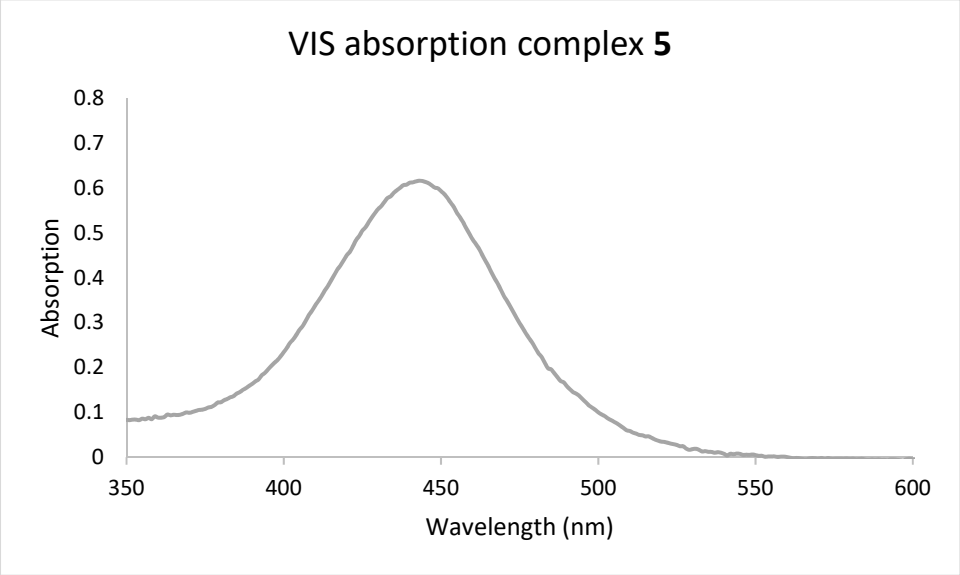

Figure S39. VIS absorption spectrum of a solution of complex **5** (3.5 μM). Calculated molar extinction coefficients: ε_{425nm}=1.4 x 10^5 M^{-1} cm^{-1} and $\varepsilon_{max(441nm)}$= 1.8 x 10^5 M^{-1} cm^{-1}.

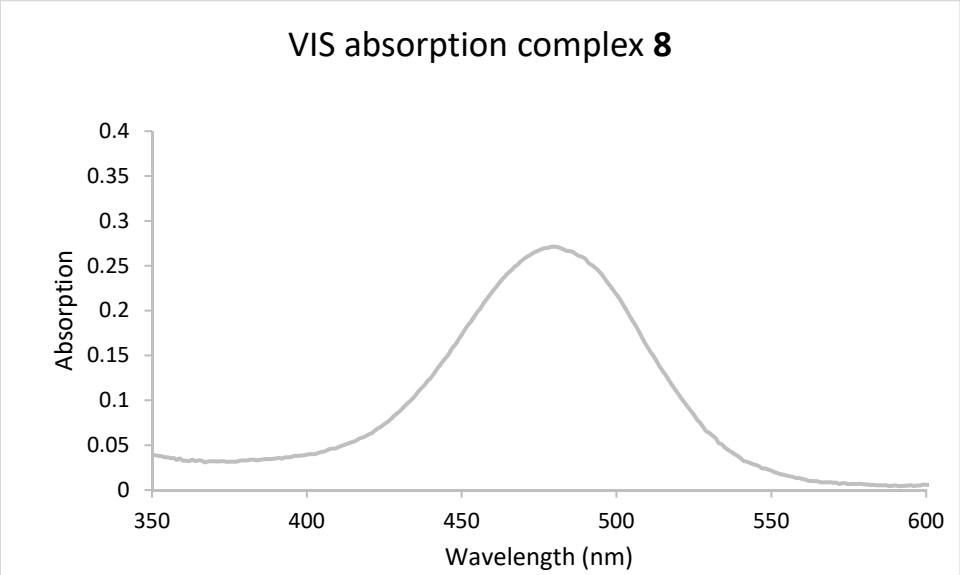

Figure S40. VIS absorption spectrum of a solution of complex **8** (1.9 μM). Calculated molar extinction coefficients: ε_{425nm}=3.9 x 10^4 M^{-1} cm^{-1} and $\varepsilon_{max(479nm)}$= 1.4 x 10^5 M^{-1} cm^{-1}.

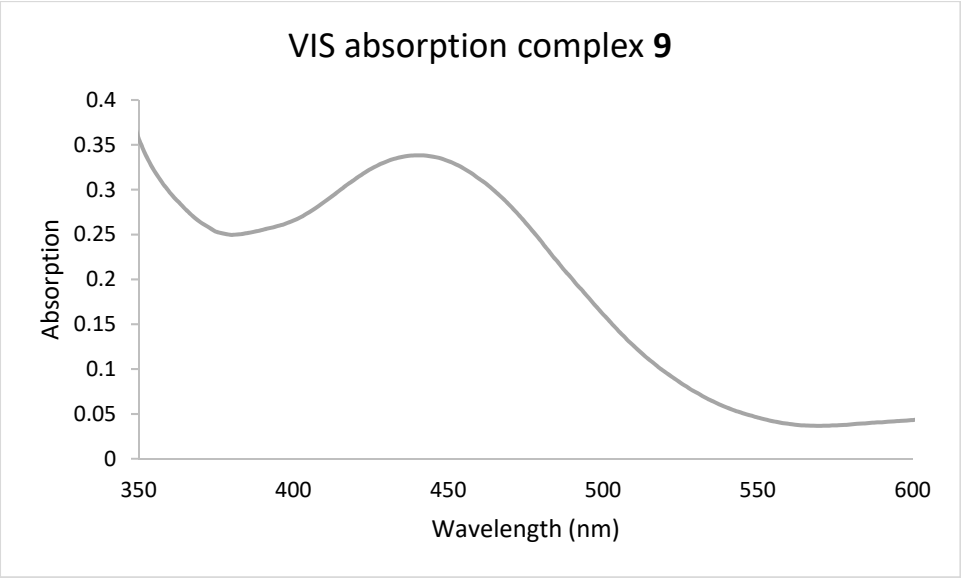

Figure S41. VIS absorption spectrum of solution of complex **9** (6.8 µM). Calculated molar extinction coefficients: ε_{425nm}=4.7 x 10^4 M^{-1} cm^{-1} and $\varepsilon_{max(441nm)}$= 5.0 x 10^4 M^{-1} cm^{-1}.

9. References

S1. G. Cecot, B. Alameddine, S. Prior, R. D. Zorzi, S. Geremia, R. Scopelliti, F. T. Fadaei, E. Solari and K. Severin, *Chem. Commun.*, 2016, **52**, 11243–11246.

S2. M. D. Wise, A. Ruggi, M. Pascu, R. Scopelliti and K. Severin, *Chem. Sci.*, 2013, **4**, 1658–1662.

S3. G. Cecot, M. Marmier, S. Geremia, R. De Zorzi, A. V. Vologzhanina, P. Pattison, E. Solari, F. Fadaei Tirani, R. Scopelliti and K. Severin, *J. Am. Chem. Soc.*, 2017, **139**, 8371–8381.

S4. N. P. E. Barry and B. Therrien, *Eur. J. Inorg. Chem.*, 2009, **31**, 4695–4700.

S5. D. P. August, G. S. Nichol and P. J. Lusby, *Angew. Chem. Int. Ed.*, 2016, **55**, 15022–15026.

S6. L. Patiny and A. Borel, *J. Chem. Inf. Model.*, 2013, **53**, 1223–1228.